High Frequency Inverter Power Stage Design Considerations for Non-Magnetic Materials Induction Cooking

Zidong Liu

Thesis submitted to the Faculty of the
Virginia Polytechnic Institute and State University
in partial fulfillment of the requirements for the degree of

Master of Science
In
Electrical Engineering

Jason Lai, Chairman
Kathleen Meehan
Wensong Yu

January 14, 2011
Blacksburg, Virginia

Key words: Electromagnetic, Induction Cooking, Series-Resonant, Soft Switching

High Frequency Inverter Power Stage Design Considerations for Non-Magnetic Materials Induction Cooking

Zidong Liu

ABSTRACT

Recently induction cookers, which are based on induction heating principle, have become quite popular due to their advantages such as high energy efficiency, safety, cleanliness, and compact size. However, it is widely known that with current technology, induction cookers require the cookware to be made of magnetic materials such as iron and stainless steel. This is why a lot of cookware is labeled "Induction Ready" on the bottom. The limited choice of "Induction Ready" cookware causes inconvenience to customers and limits the growing popularity of the induction cooker. Therefore, a novel induction cooker, which can work for non-magnetic material cookware such as aluminum and copper, can be very competitive in the market.

This thesis studies the induction cooking application; briefly introduces its fundamental principle, research background and the motivation of the development of a non-magnetic material induction cooker. Followed by the research motivation, three commonly used inverter topologies, series resonant inverter, parallel resonant inverter, and single-ended resonant inverter, are introduced. A comparative study is made among these three topologies, and the comparative study leads to a conclusion that the series resonant inverter is more suitable for non-magnetic material induction cooking application.

The thesis also presents several major issues about non-magnetic material induction cooking and how to deal with these issues through induction coil design, higher operating frequency and novel control strategy. Because of non-magnetic material's low resistivity and permeability characteristics, it is difficult to be heated and to achieve soft-switching while the coupling between the induction coil and the cooking pan can be easily changed. Later in this thesis, these issues will be discussed in detail and some potential solutions to these issues such as self-sustained oscillating control, optimized induction coil design, proper selection of power semiconductor device, etc.

A 1.5 kW high frequency series resonant inverter with self-sustained oscillating control is prototyped. Experimental results demonstrated successful operation of the resonant inverter under up to 1.5 kW, and the inverter's capability to maintain zero-voltage turn-on during wide operating condition is confirmed.

At the end, a summary is given about the research work done in the thesis and future research work is discussed.

ACKNOWLEDGEMENTS

First, I would like to express my deepest gratitude to my advisor, Dr. Jason Lai, for his kind guidance, advice and support during my study at Virginia Tech. He was nice and eager to help me solve many technical problems encountered throughout my research.

I would also like to thank Dr. Huang-Jen Chiu from Taiwan University of Science and Technology, for his kind help and valuable advice during his one year visit at Virginia Tech.

In addition, I am very grateful to Dr. Wensong Yu, Yuzha Chen, Hongmei Wan, Cong Zheng, Alex Kim, Thomas LeBella, Daniel Martin, and all FEEC members for their helpful guidance, discussion, support on course work and research, and for maintaining a joyful, amicable and stimulating research atmosphere. Without their support, encouragement and guidance, this thesis would not be completed.

Finally, I must thank the support from my parents and brother for their years of encouragement and support in every stage of my life.

TABLE OF CONTENTS

LIST OF TABLES AND FIGURES

Chapter 1 Introduction

1.1 Research Background and Motivation

The first induction cooker was introduced at the Chicago World's Fair in 1933. [27] From then on, induction cooker has become quite popular in Europe and several East Asian nations with approximately 60%-70% penetration rate. In the United States, induction cooker is also becoming popular due to its advantages such as fast heating, high thermal efficiency, safety, compact size, and cleanliness.

The thermal efficiency of an induction cooker is significantly higher than that of other cooking methods such as gas or an ordinary electric cooker because energy is transmitted to the cooking pan directly by magnetic field without dissipating any heat into the surrounding environment. With gas or ordinary electric cookers, energy is converted into heat first and then used to heat the cooking pan, leading to a significant amount of waste heat and low thermal efficiency. According to Table 1.1, only 25-30% of energy in standard gas and 30-40% of energy in High Efficiency Gas are used for cooking, and with induction cooking around 80-90% of energy in electricity gets used for cooking. The table below shows several efficiencies from different sources.

	Range Top Energy Efficiency
High Efficiency Gas (%)	30-40
Standard Gas (%)	25-30
Electric (%)	60-65
Induction (%)	80-90

Table 1.1 Range Top Energy Efficiency

In addition, induction cookers will not produce flames or any wasted gas. The unit's surface stays cool and doesn't burn the user's fingers when touched. It is easy to clean since the unit's surface is flat.

Despite having so many advantages, the induction cooker has one major drawback which is the limited selection of "Induction Ready" cookware. With current technology the induction cooker only works with cookware made of magnetic materials such as iron and stainless steel which causes a lot inconvenience to the customer. Therefore, the development of a novel non-magnetic material induction cooking technology would further increase the product's market competence.

A non-magnetic material induction cooker has several advantages such as low cost of aluminum for the cooking pan and the aluminum pan has excellent thermal conductance. By using an aluminum cooking pan, the heat can spread to all areas of the cooking pan evenly and cook the food without overheating and hotspots. The last benefit is that more than 50% of cooking pans in the market are made of aluminum. Therefore the customer will have more selection of cooking pans.

1.2 Thesis Outline and Major Results

Below is an outline of the thesis:

Chapter One:

The first chapter introduces some advantages of the induction cooker such as high thermal efficiency, safety, and cleanness. In addition, the motivation of non-magnetic material induction cooking is briefly introduced.

Chapter Two:

This chapter explores the fundamental principle of induction cooking and the induction cooking load characteristics are modeled. The research problems for non-magnetic material induction cooking are also presented. Solutions such as optimized induction coil design, proper selection of power semiconductor devices, and a novel control scheme are suggested. The overview of several inverter topologies widely-used in induction cookers is introduced and each inverter topology is analyzed. A comparison between those inverter topologies is performed. After the comparative study, the conclusion was drawn that the half bridge series resonant inverter is more suitable for non-magnetic induction cooking.

Chapter Three:

In this chapter a half bridge series resonant inverter with self-sustained oscillation control scheme is proposed and analyzed in detail.

Chapter Four:

A 1.5 kW non-magnetic induction cooker power stage is prototyped. The experimental result confirms that with the proposed self-sustained oscillating control, the inverter power stage can operate safely up to 1.5 kW and maintain zero-voltage turn-on while the inverter's resonant frequency is constantly changing. This chapter also discusses several other control schemes such as triple resonant frequency control, DC-link voltage control and the combination of fundamental resonant frequency, triple frequency, and quintuple frequency control.

Chapter Five:

A thesis conclusion is presented and potential future research work is provided for non-magnetic induction cooking.

Chapter 2 Induction Cooking Overview

2.1 Principle of Induction Cooking

Induction cooking is an application of induction heating, which converts electrical energy into heat based on the principle of electromagnetic induction. As shown in Figure 2.1, inside an induction cooker an induction coil is placed underneath the cooking pan. [5] While an AC current generated by the high frequency inverter flows through the induction coil, the induction coil will produce a high-frequency electromagnetic field. The electromagnetic field penetrates the bottom of the cooking pan and sets up an eddy current which generates Joule heat. Therefore, for induction cooking, the heat is generated in the cooking pan directly and is then transferred to the pan's contents. No heat is dissipated outside the pot during the electrical-heat transfer process.

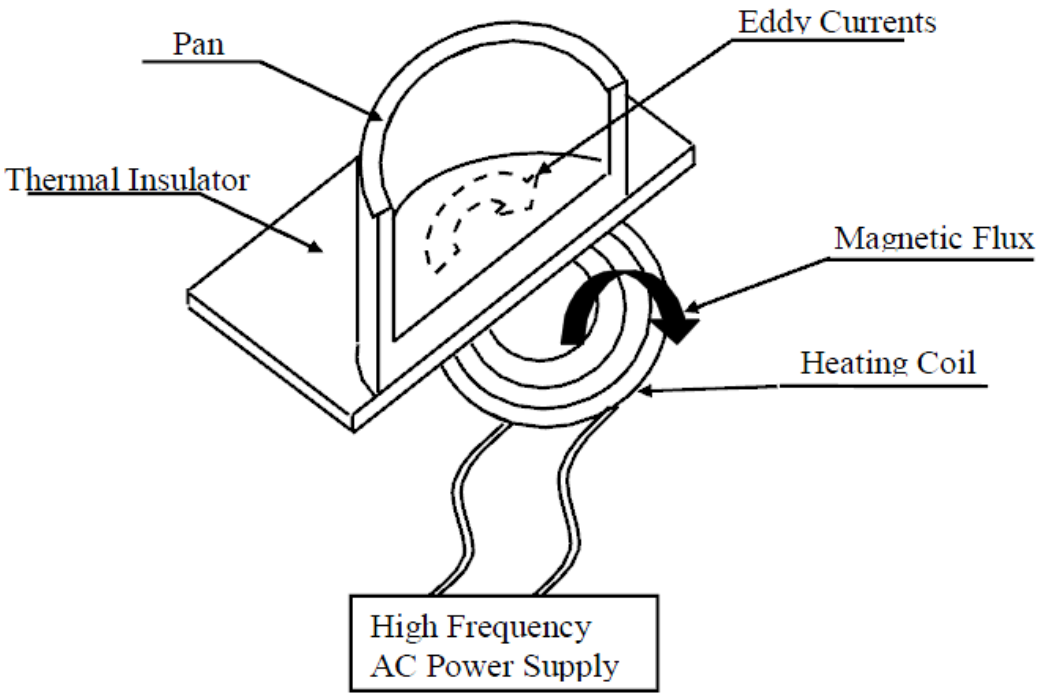

Figure 2.1 Principle of Induction Cooking

2.2 Induction Cooking Load Characteristics

While a cooking pan is placed on top of an induction coil as shown in Figure 2.2, it can be redrawn in the form of a transformer as shown in Figure 2.3. The induction coil is actually a planar inductor. In this case, while a cooking pan sits on top of it, the induction coil then can be considered as an air core transformer's primary winding with N number of turns. Since the magnetic field generated by the induction coil will penetrate the bottom of the cooking pan and set up an eddy current as shown in Figure 2.1, the cooking pan would behave as its closed secondary winding as shown in Figure 2.3 with the number of turns 1. The resistance of the induction coil, R_{coil}, changes with frequency due to skin effect, proximity effect, and the change in temperature. L_{coil} is the self-inductance of the induction coil. L_m represents the mutual inductance between the induction coil and cookware. R_{eff} is the effective resistance of the cooking pan when reflected back to the induction coil side.

Figures 2.2-2.5 show the step-by-step derivation of the equivalent inductance and resistance for the induction coil coupling with a cooking pan. Figure 2.2 shows the schematic of the induction coil coupling with the cooking pan on top of it. Figure 2.3 redraws the schematic in the form of an air-core transformer. Figure 2.4 further derivates the schematic in detail by defining coil resistance, effective load resistance, leakage inductance, and magnetizing inductance respectively. Figure 2.5 finally simplifies the schematic into a form of an equivalent resistance in series with an equivalent inductance

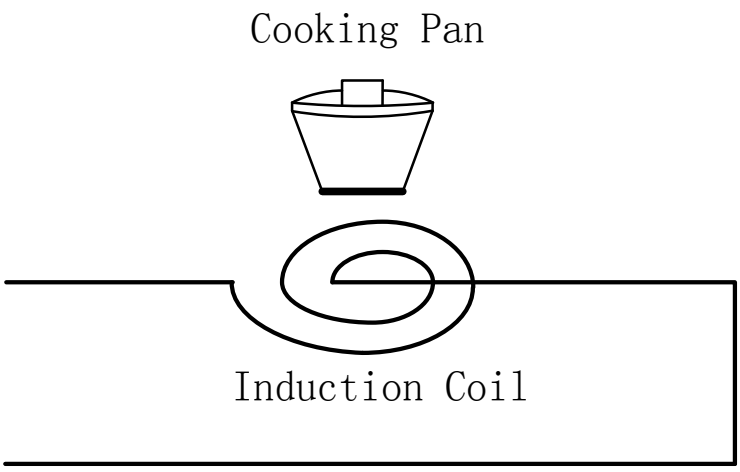

Figure 2.2 Induction Coil with Cooking Pan

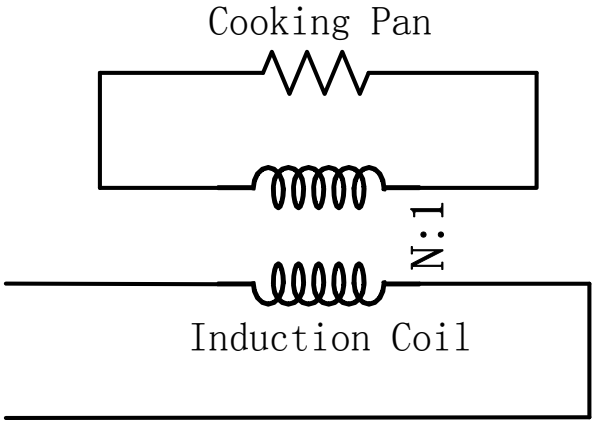

Figure 2.3 Induction Coil with Cooking Pan in the Form of Transformer

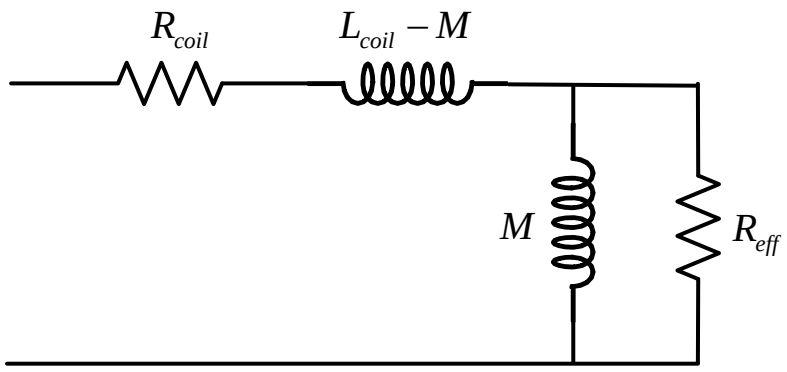

Figure 2.4 Induction Coil with Cooking Pan Model 1

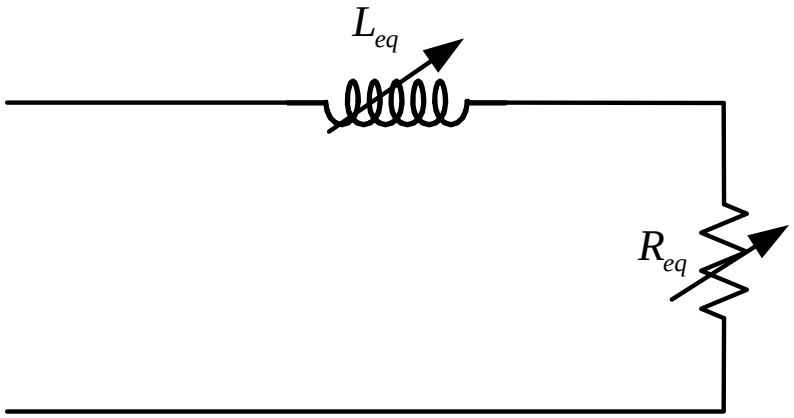

Figure 2.5 Induction Coil with Cooking Pan Model 2

The induction coil and the cooking pan (load) can be represented by an equivalent series combination of R_{eq} and L_{eq}, where the values of R_{eq} and L_{eq} are as follows.

$$R_{eq} = R_{coil} + \frac{\omega L_M}{\sqrt{R_{eff}^2 + \omega^2 L_M^2}} R_{eff} \qquad (2\text{-}1)$$

$$L_{eq} = L_{coil} - \frac{\omega L_M}{\sqrt{R_{eff}^2 + \omega^2 L_M^2}} L_M \qquad (2\text{-}2)$$

2.3 Characteristics of Non-Magnetic Material Cooking Pan

As previously explained, the induction cooker transfers the energy by producing an electromagnetic field and generating eddy currents on the bottom of the cooking pan. Thus the energy is dissipated as heat, causing the cooking pan—and by conduction, its contents—to become hot. The heat dissipation caused by the eddy current is called Joule heat in this thesis.

In addition to Joule heat, magnetic materials such as iron and steel can also be heated by hysteresis loss. Normally its magnetic domains within the material are randomly oriented. As the magnetic field is applied, it exerts force upon the magnetic domains within the material and causes the magnetic domains to align in the same direction. As the magnetic field flips polarity, the domains flip polarities too and create friction which produces heat. The energy lost through hysteresis depends on the strength of the magnetism in the material and the area of the hysteresis loop as shown in Figure 2.6. [28] The hysteresis loop is a plot of the magnetic field versus the magnetic energy density for a material. An illustration of the flipping of magnetic domains is in Figure 2.6 below. Hysteresis is important for induction cooking as it is the dominant source of heating. The losses due to hysteresis are usually a secondary effect in most industrial applications because Joule heating is dominant.

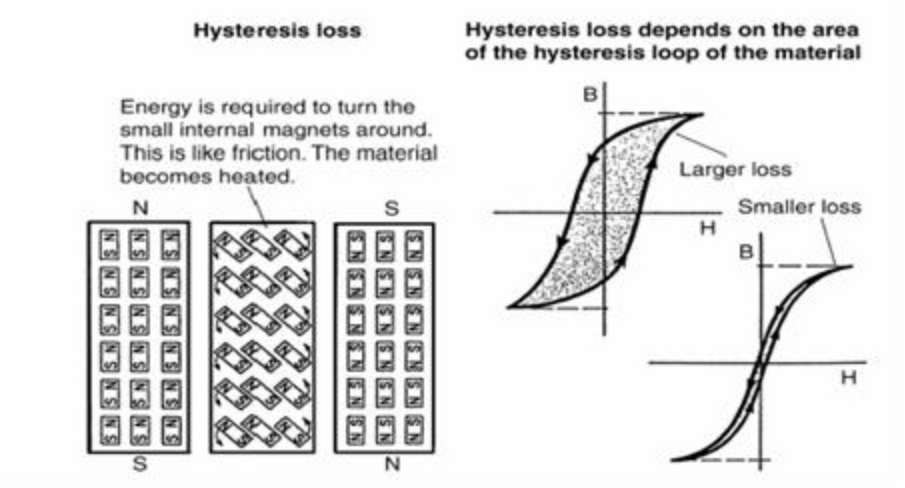

Figure 2.6 Hysteresis losses due to magnetic domains of ferromagnetic materials

Because non-magnetic material such as aluminum and copper cannot be magnetized, no hysteresis loss will be generated and only Joule heat can be used to heat up this kind of material. This is one reason why non-ferrous material is difficult to heat up by induction.

Another issue is that non-magnetic material such as aluminum and copper has low resistivity and permeability. As shown in Figure 2.5, the equivalent resistance is a combination of induction coil ESR and the effective load resistance. Therefore, in order to transfer the energy to the load without dissipating inside the induction coil, the effective load resistance must be significantly greater than the induction coil ESR. For magnetic material such as iron and stainless steel, since their resistance and permeability is much higher than that of the induction coil, which is typically made of copper, most energy will be used to heat up the cooking pan (load). For non-magnetic material such as aluminum and copper, since their resistance and permeability is the same as induction

coil, a significant amount of energy would be dissipated in the induction coil. Therefore, the first issue with non-magnetic material induction cooking is how to increase its resistance.

Material	Iron	Non-magnetic Stainless Steel	Aluminum	Copper
Resistivity ρ (Ω-m)	9.8×10^{-8}	70×10^{-8}	2.8×10^{-8}	1.7×10^{-8}
Relative permeability μ_r	100	1	1	1
Skin depth δ (mm) at f=20kHz	*0.11*	2.9	0.59	0.46
Surface resistance R_s *(Ω) at f=20kHz*	8.8×10^{-4}	2.3×10^{-4}	0.47×10^{-4}	0.37×10^{-4}

Table 2.1 Characteristic of different pot materials

As shown in Table 3.1, because aluminum and copper are non-magnetic material, their relative permeability ρ and resistivity R_s are very small. Therefore, it is difficult to heat up an aluminum or copper pan. Although the 18-8 stainless steel is also a non-magnetic material and has a large skin effect depth value δ, it has a relatively large relative permeability ρ and R_s, therefore it can be suitable for ordinary induction cooking similar to an iron pan.

Overall, comparing aluminum with iron under the same condition f=20 kHz, aluminum's relative permeability is 1/100 of irons and its resistivity is 1/3.5 of irons. Therefore, aluminum's effective resistivity is 1/19 of irons. In other words, by using the same induction coil and applying the same amount of AC current, the energy dissipated into aluminum is just 1/19 of iron's.

Generally speaking, for an ordinary induction cooker to heat up the iron pan, the induction coil's number of turns should be set around 15~ 20 and the operating frequency can be designed at around 20 kHz. If we want to heat up the aluminum or copper pan, the prerequisite is that their effective resistance needs to be increased to the same value of iron pan.

2.4 Major Issues and Potential Solutions for Non-Magnetic Material Induction Cooking

The input resistance Z_{in} of an induction coil, shown in Eq. 2-3, is proportional to the square of the number of induction coils, and it can be expressed as

$$Z_{in} = K \times n^2 \times R_s + R_c \qquad (2\text{-}3)$$

Where K is a coefficient constant that depends on the shape of both the induction coil and cooking pan;

n is the induction coil's number of turns;

R_C is the induction coil's ESR resistance;

R_S is cooking pan's surface resistance;

According to Eq. 2-3, we can say the input resistance can be increased by the following methods.

First, the induction coil's number of turns can be increased because by Eq. 2.3 the input resistance is proportional to the square of the number of turns, n. However, any increase in the number of turns will inevitably lead to an increase in the induction coil's self-inductance. In the next chapter, the issue associated with large self-inductance will be discussed.

Second, the load surface resistance can also be increased as higher operating frequency increases due to the skin effect. The skin effect causes the current distribution to be uneven through the cross section of the cooking pan's bottom. Actually at high frequency, the eddy current distribution decreases exponentially as depth increases. At a certain depth, the current decreases to 36% of the surface current value. This depth is called the penetration depth and is defined as shown in Eq. 2-4

$$\delta = \sqrt{\frac{1}{4\pi^2 \times 10^{-7}}} \sqrt{\frac{\rho}{f \bullet \mu_r}} \qquad (2\text{-}4)$$

Where δ is the penetration depth;

ρ is the resistivity;

f is the frequency;

μ_r is the relative permeability.

Due to the skin effect, the high frequency current tends to be highest at the surface of a conductor and then to decay exponentially toward the center. In other words, the

skin effect causes the effective cross sectional area to decrease. Since the resistance of a conductor is inversely proportional to the cross sectional area of the conductor, the resistance can be increased while the cross sectional area decreases by Eq. 2-4,

At high-frequency due to skin effect, the cooking pan's surface resistivity R_s can be expressed in Eq. 2-5.

$$R_s = \frac{p}{\delta} = \sqrt{4\pi^2 \times 10^{-7}} \sqrt{f \mu_r p} \qquad (2\text{-}5)$$

In addition, Litz wire can be used to reduce the skin effect and proximity effect on the induction coil. A Litz wire typically consists of hundreds of thin wire strands, which are individually insulated and then twisted together. Because each thin wire strand is less than a skin-depth, the impact of skin effect is negligible to each individual strand. Furthermore, because those strands are twisted together, each individual strand will reside for a short interval on the outside of the wire and for short interval on the inside of the wire so it can effectively reduce the skin effect and proximity effect. According to the skin effect theory, the inside of Litz wire suffers from a stronger electromagnetic field and higher resistance than the outside of wire. By twisting strands together, each strand sees about the same average resistance, and then each strand will contribute equally to the conduction of the entire wire.

Third and finally, the resistance can be increased by better coupling between the induction coil and the cooking pan according to Eq. 2-1.

2.5 Limitation to Increase Non-Magnetic Material's Resistance

As discussed previously, the output power can be transferred into the cooking pan by the following ways;

(1) Increase of operating frequency in induction coil

(2) Increase of induction coil's number of turns

(3) Increase the coupling between the cooking pan and the induction coil

However, the increase of induction coil's number of turns results in high coil inductance. According to Sebastiaan's formula for a flat "pancake" coil in Eq. 2-5, the coil inductance is proportional to the square of induction coil's number of turns.

$$L \approx \frac{(NR)^2}{8R + 11W} \qquad (2\text{-}6)$$

Where N is the induction coil's number of turns

R is the distance from the center to center of windings in inches

W is the width of windings in inches

Below shows three induction coils with different numbers of turns and their respective inductance values which confirms Sebastiaan's formula.

Figure 2.7 Induction Coil with 32 turns and 147uH inductance

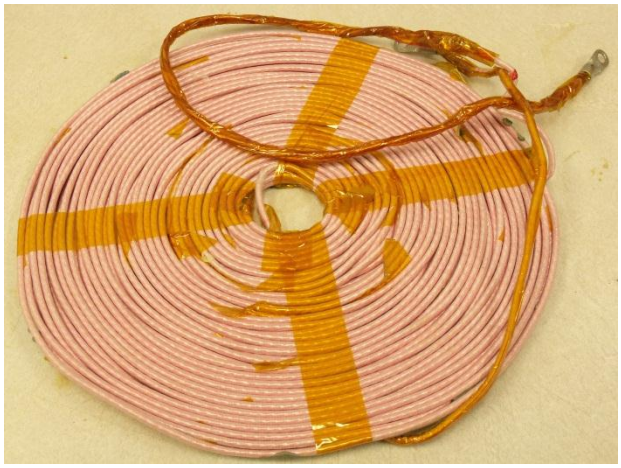

Figure 2.8 Induction Coil with 60 turns and 473uH inductance

Figure 2.9 Induction Coil with 96 turns and 1.126mH inductance

For the series resonant inverter, its quality factor is expressed in Eq. 2-7.

$$Q = \frac{1}{R}\sqrt{\frac{L}{C}} \tag{2-7}$$

By Eq. 2-7, assume the cooking pan's surface resistance is 3Ω and the inverter's operating frequency is at 100 kHz, then the quality factor can be obtained.

Load Resistance	Inductance	Capacitance	Quality Factor Q
3Ω	147uH	17.25nF	30
3Ω	473uH	5.36nF	90
3Ω	1.126mH	2.25nF	236

Table 2.2 Quality Factor for Different Induction Coil

In order to make the resonant frequency unchangeable at around 100 kHz as the coil inductance increases, the resonant capacitor must be decreased to a smaller value. Therefore, with a large inductor and a small capacitor, we have a high Q system. By Eq. 2-8, at the resonant frequency, the voltage stress on each resonant element L_r and C_r is equal to the quality factor multiplied by the DC-link voltage. Due to this reason, the

induction coil's number of turns cannot be increased without a limit. If the induction coil's inductance is too large, the resonant voltage on each resonant element may easily exceed 10kV and cause an electric arc issue.

$$V_{C_r} = V_{L_{eq}} = QV_S \tag{2-8}$$

Another issue for non-magnetic material is that it cannot conduct magnetic flux. Referring to Figure 2.4, the resonant inductor is actually determined by induction coil's leakage inductance and magnetizing inductance by Eq. 2-2. Table 2.3 shows that for non-magnetic material, its coupling factor will change with different pan size, or by moving and lifting the pan during the cooking process. As the resonant inductance changes with a fixed resonant capacitance, the inverter's resonant frequency will also change. As explained in a later chapter, the switching frequency must be greater than the resonant frequency in order to maintain a zero-voltage turn-on (ZVS) condition. Therefore, frequency tracking control is a must for this type of application.

Figure 2.10 Cooking Pans with Different Size

1.094mH	Small → Large			
Center ↓ Border	Pan#1	Pan#2	Pan#3	Pan#4
	711μH	603μH	395μH	402μH
	725μH	685μH	460μH	464μH
	812μH	755μH	538μH	673μH
	887μH	839μH	638μH	830μH

Table 2.3 Variation of Inductance vs. Pan Size and Location

Also according to the skin effect theory, the overall thermal efficiency can be increased by simply pushing the operating frequency higher. However, there is always a limitation on the maximum operating frequency a certain type of power semiconductor device can handle since higher operating frequency always leads to higher switching loss by Eq. 2.8.

$$P_{loss\ sw} = (E_{on} + E_{off}) f_s \tag{2-8}$$

Typically, a switching loss occurs when a power device changes from one state to another state. For example, Figure. 2.10 shows a Bipolar Junction Transistor (BJT) switching from the off state to the on state. Initially, when the device is in the off state, V_{CE} is high and I_S is zero. At the hard switching turn on moment, first the current rises to

the operating value and then V_{CE} drops to close to zero. The overlap between the voltage and current creates a large switching loss.

Conduction loss is another major source of loss that needs to be considered. The conduction loss varies depending on the type of power semiconductor device. For example, while a MOSFET is turned on, it can be considered as an equivalent resistor $R_{ds(on)}$, which varies its value under different temperature conditions. Junction type power device such as BJTs and IGBTs have different conduction loss characteristics. For example, while an IGBT is turned on, the voltage drop across it can be considered fairly fixed. The power loss can be easily determined by multiplying the conducting current with the voltage drop.

2.6 Soft-switching Technology

Higher energy conversion efficiency at high switching frequencies can be obtained by manipulating the voltage or current at the moment of switching to become zero. This is called "Soft Switching". Soft-switching can be categorized into two types, ZVS turn-on and ZCS turn-off, and is very important in induction cooking applications. As mentioned previously, by increasing the switching frequency we can increase the cooking pan's surface resistance and be able to transfer the output power into the cooking pan. However, as we push the switching frequency higher, the switching loss will always transfer into the form of heat and excessive heat may damage the power semiconductor device and make the device reliability a major issue. Because semiconductor devices are not entirely ideal, as the switching frequency increases, high-frequency noise and switching losses increase.

It is common sense that if you force the device switching while there is still energy stored inside the device, such as the minority carrier charge stored in the base region for a BJT or the accumulated charge stored in the output capacitor for a MOSFET, the energy must be converted into heat and other forms of electromagnetic energy and can cause switching losses if the energy has nowhere to go. Then we have soft switching technology to solve the issue. The main principle of soft switching is to transfer the energy stored inside the device to other storage devices such as inductors and capacitors before the switching action even takes place by LC resonance, auxiliary switches, or other methods.

Three popular semiconductor devices, power bipolar junction transistors (BJTs), metal oxide field-effect transistors (MOSFETs), and insulated gate bipolar transistors (IGBTs), will be introduced and compared. In order to select the appropriated power semiconductor device, a comparative study must be done and their advantages, disadvantage and trade-offs must be considered for non-magnetic induction cooking applications.

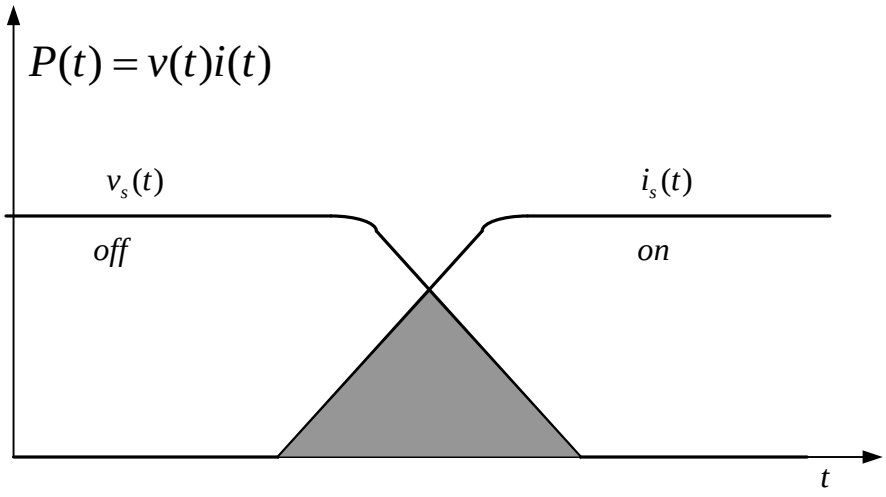

Figure 2.11 Turn-off Loss of Bipolar Junction Transistor

2.7 Comparative Study of Power Semiconductor Devices

First, a BJT is a current controlled, minority carrier device, and typically has lower conduction loss than a MOSFET due to the conductivity modulation. Because of its unique characteristics, it can be used for high current applications, but it requires much more complex drive circuitry due to its low input impedance current-control characteristics. In addition, when the BJT is forward biased, minority carriers accumulate in the p and n regions near the junction. In the p region there is accumulation of electrons and in the n region accumulation of holes. These accumulated charges are separated by the depletion region which can be considered as a capacitor. This capacitance is called minority carrier. As forward current increases in the base, more charge accumulates and the depletion region becomes thinner. As a result the capacitance increases and the stored minority carrier charge must be removed before the transistor is turned off. This turn off process is slower compared to a MOSFET's turn off

time. The BJT is a much slower device than a MOSFET generally due to this longer turn off time. Since the turn-off process is slower, device current will flow as voltage is present across the device; ultimately resulting in greater switching loss. Lastly the BJT has a negative temperature coefficient, which means that the device cannot be used in parallel with other BJTs to further reduce conduction loss.

The metal oxygen field-effect transistor (MOSFET) is a voltage-controlled, majority carrier device. It has high input impedance and requires significant low current to drive it. The drawback is that it has a relative higher conduction resistance $R_{ds(on)}$ for high breakdown voltage rated devices. This results in higher conduction loss at high breakdown voltage, which limits its current carrying capability. Even though the MOSFET has superior turn-off performance, it also has an undesirably large parasitic output capacitance. When the switch is in the off state, charge will accumulate in the output capacitor C_s. The total energy stored inside the output capacitor is equal to $\frac{1}{2}C_s^2V_s^2$, where V_s is the voltage across the output capacitor before the MOSFET is turned on. At the switch's turn-on moment, the output capacitor will release the energy, resulting in large current spike. Since the device is not designed to handle such large current spike, the device may be damaged during the turn-on transient by the current spike.

In general, MOSFETs has the following advantages over BJTs. The first advantage is that it requires simple drive circuitry due to high input impedance and low required driving current to the device on and off. The second one is faster switching speed. The last one is because the MOSFET has a positive temperature coefficient; it can be paralleled with other MOSFETs to further decrease conduction loss. The drawback for MOSFET is that it has high conduction loss and low current carrying capability.

The BJT usually can be considered a slow device due to the slow turn off time and is difficult to drive; however, because of its ability to provide high currents and withstand high voltages, the BJT is usually chosen for use in high power, high current applications.

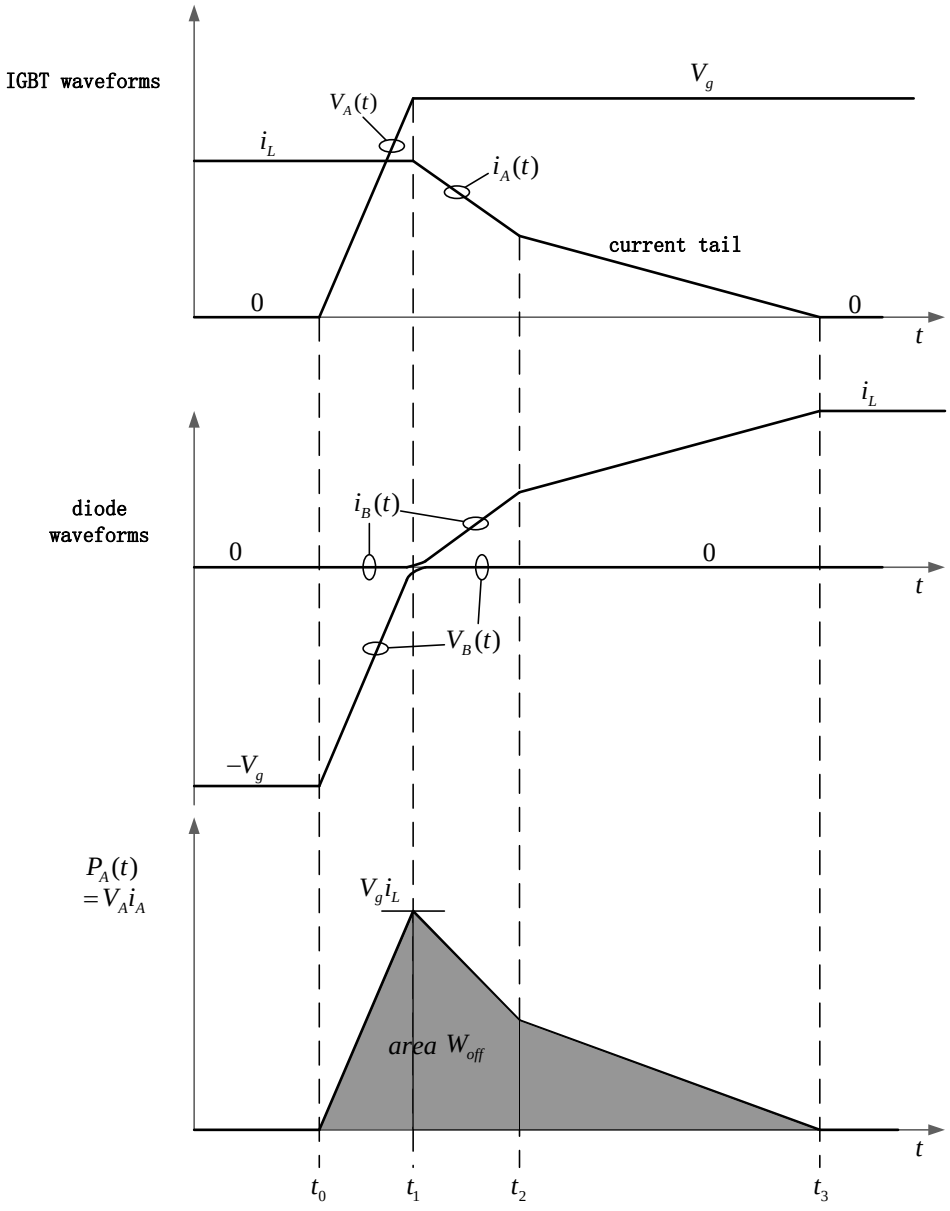

Figure 2.12 IGBT Turn-off Switch Realization

The IGBT was invented as a new semiconductor power device that combines an easily driven MOS gate of a MOSFET and low conduction loss characteristic of a BJT. The balance in tradeoffs between switching speed, and conduction loss makes IGBT become a popular device for high frequency (below 100 kHz), high current and high voltage applications. In this thesis, the Fairchild IGBT HGTG20N60A4D is chosen for the induction cooking application. Table 2.4 shows a comparison between IGBT and MOSFET.

	MOSFET	**IGBT**
DRIVE CIRCUITRY	SIMPLE	SIMPLE
DRIVE POWER	LOW	LOW
SWITCHING SPEED	FAST	MEDIUM
BREAKDOWN VOLTAGE	Medium	High
ON-RESISTANCE	HIGH	LOW
DEVICE PARALLELING	YES	NO

Table 2.4 Comparison between MOSFET and IGBT

Similar to the BJT, the IGBT also can be considered difficult to turn off due to the minority carrier charge stored in its base region. As shown in Fig. 2.11the device has a tail current which overlaps voltage during device turn off, resulting in significant turn off loss. A study has been completed on switching loss comparison for the IGBT between hard-switching, ZVS turn-on, and ZCS turn-off condition [26]. Due to the IGBT's tail current, it is very difficult to completely eliminate the IGBT's turn-off loss. Comparing ZCS turn-off with ZVS turn-on, the latter works better; a snubber capacitor can also be used to further reduce the IGBT's turn-off loss.

2.8 Conclusion

This chapter explains because of non-magnetic material's low resistivity and permeability characteristics, it is difficult to be heated. Next, three options are introduced to increase non-magnetic material's resistivity. In order to heat up a non-magnetic material pan, one option is to increase the operating frequency to match the magnetic material's surface resistivity by the Skin Effect. However higher switching frequency will undoubtedly cause higher switching loss, which leads to reduced power efficiency and device reliability. In addition, due to the IGBT's tail current phenomenon, current high power IGBT can only handle a switching frequency up to 100 kHz. Another option is to increase the number of turns on the induction coil. As explained an increase of the number of turns on the induction coil causes high voltage stress on resonant elements, which leads to electrical arcing problems. The last option is to increase the coupling between the cooking pan and the induction coil. Since non-magnetic material cannot conduct magnetic flux, it is very difficult to improve the coupling. In addition, since the coupling factor is not fixed the resonant inverter needs frequency tracking control in

order to maintain the zero-voltage turn-on (ZVS) condition as resonant frequency changes.

Chapter 3 Induction Cooking Inverter Topology and Control Study for Non-Magnetic Cooking Pans

3.1 High Frequency Induction Cooking Inverter Topology and Control Study

In this chapter, three commonly-used soft-switching inverter topologies for induction cooking are introduced and a comparison among them is performed.

3.1.1 Voltage-Fed Series-Resonant Inverter

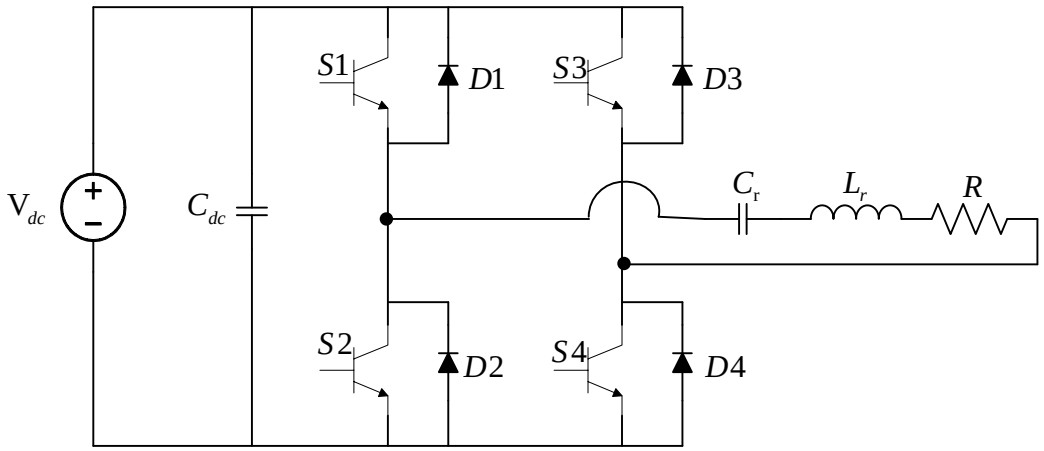

Figure 3.1 Series Resonant Inverter

The full bridge type series resonant inverter topology is shown in Figure 3-1. L_r represents the resonant inductor, which is modeled by Eq. 2-2. C_r represents the resonant capacitor. This is called series resonant inverter because the load is in series with the resonant tank, which is formed by the resonant capacitor and resonant inductor. This circuit has the following characteristics:

(1) As shown in Fig 3.1, the voltage stress applied on the switching device is just the DC-link voltage while the switch is turned off. The resonant current is a sinusoidal wave. For inverter operation above the resonant frequency, the resonant current will flow

through the anti-parallel diode before the switch is turned on. During the device turn on instant the voltage applied across the device is just the anti-parallel diode's forward voltage, which is typically a very low value and we say the inverter is operating in the ZVS condition. Today most semiconductor device companies offer high power switching device such as MOSFETs and IGBTs with an integrated anti-parallel diode (2) The series resonant inverter can be controlled by self-oscillating signal or IC-controlled signal. However, if the IC-controlled signal is far away from the resonant frequency, efficiency will be low. An increase in reactive current and a decrease in real output power may cause a serious heat issue for power devices.

(3) The series resonant inverter's resonant capacitor requires a high voltage rating. For a high quality power system, the inverter may require multiple capacitors in series for a high voltage rating.

(4) As a voltage fed inverter, it is possible to have short-circuited while the upper device and lower device are turned on simultaneously. Since the voltage across dc-link capacitor cannot change abruptly, instantaneous discharging current will be very large and far beyond the power device current rating. If the device is not turned off within the time allowed for short circuit fault, it will cause permanent damage to the device. The circuit must be protected against short-circuit fault with a fast current sensor and a driver IC with a short-circuit protection feature.

3.1.2 Current-Fed Parallel resonant inverter

The parallel resonant inverter topology is shown in Figure 2-7. The equivalent series inductor and resonant capacitor are in parallel to form the resonant tank. It is defined as parallel resonant inverter because the load is in parallel with the resonant capacitor. This circuit has the following characteristics:

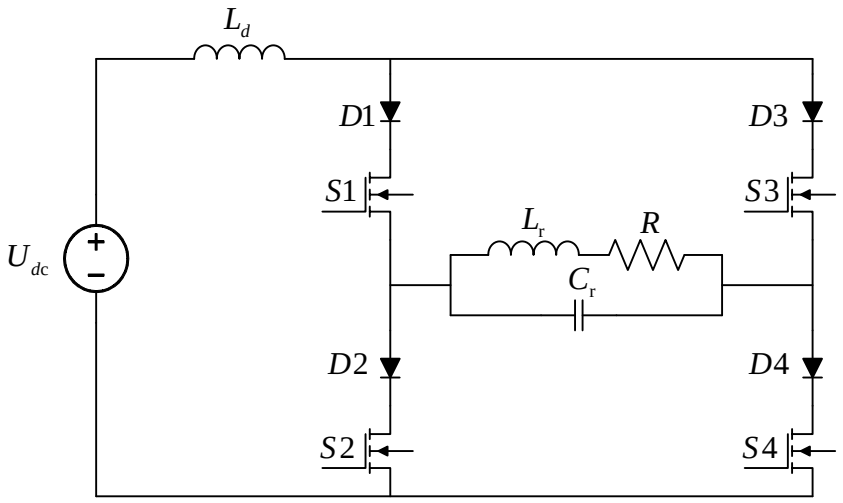

Figure 3.2 Parallel Resonant Inverter

(1) Because the resonant tank is constituted by the resonant inductor and resonant capacitor in parallel, it has a load insensitivity characteristic. This means that the current carried by the power device and resonant components is relatively independent of the load.

(2) While parallel resonant inverter is operating above resonance, it can be operated in ZCS. Vice versa, if it is operating below resonance, it can be operated in ZVS.

(3) Each switch consists of a power semiconductor device in series with a fast recovery diode. This series diode disables the internal body-drain diode of the power

semiconductor device that would normally allow negative current to flow when the switch is off. However, the fast recovery diode must have the same voltage rating as the power semiconductor device. Today such a fast recovery diode with high voltage and high current rating is usually very expensive. In addition, the fast recovery diode would inevitably increase the conduction loss.

(4) Parallel resonant inverter is current-fed and has a large input inductor. Because the inductor's current cannot change abruptly in the short circuit condition, it naturally limits the current rising slope and makes it easy to implement short-circuit fault protection. This inductance will be very large in size, thus increasing the volume of the entire unit.

(5) As shown in Fig. 3.2, inverter's input inductor can be considered as a current source. So when the upper device and lower device are turned off at the same time, the energy stored inside the large input inductor has nowhere to go. This results in a huge voltage stress across the bridge and could result in permanent damage to the devices.

(6) Parallel resonant inverter does not require a very high voltage rating for the resonant capacitor, as long as it can withstand the peak value of the input voltage. Such a capacitor is relatively cheap and can be easily found on the market.

3.1.3 High frequency Single Ended Type ZVS Inverter Power Stage Time Domain Analysis

A Single Ended Type ZVS soft-switching high-frequency inverter is probably the most widely used topology for induction cooking due to its low cost and simplicity. In

addition, the topology can track the resonant frequency and achieve soft switching in a relatively easy way.

, since the coupling factor between the cooking pan and the induction coil is not fixed for non-magnetic material induction cooking as stated in Chapter 2, the resonant inverter needs frequency tracking control in order to maintain ZVS condition as resonant frequency changes. Therefore it is worth studying how single ended type ZVS inverter controls the output power and implementation of frequency tracking to achieve ZVS by time domain analysis.

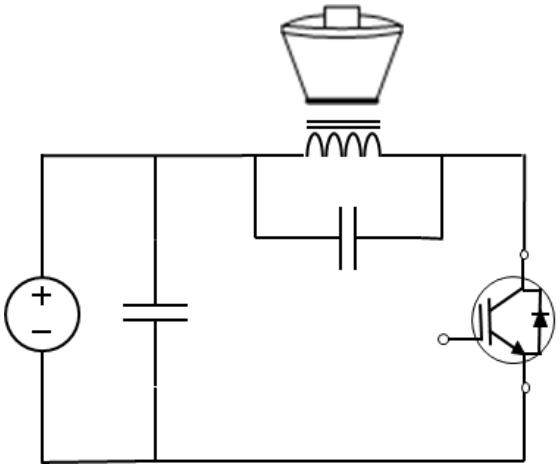

Figure 3.3 Single Ended Type ZVS Resonant Inverter

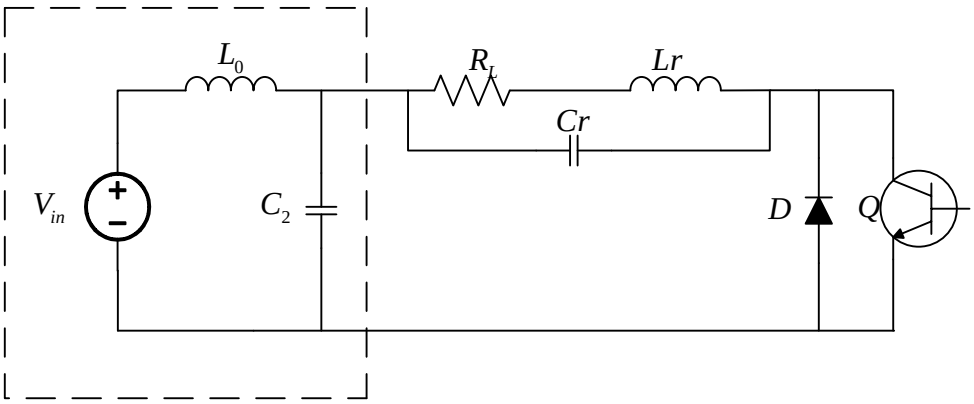

Figure 3.4 Schematic of Single Ended Type ZVS Resonant Inverter

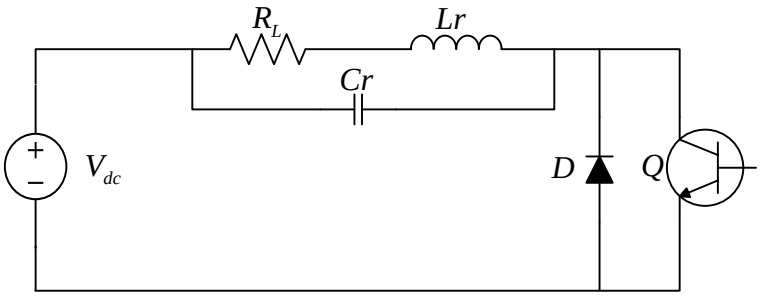

Figure 3.5 Simplified Single-Ended ZVS Inverter

Fig. 3.4 shows a schematic of single ended type ZVS resonant inverter with an input filter network constituted with input capacitor C_2 and input inductor L_0. The inverter power stage can be redrawn in terms of equivalent series inductor and resistor, as shown in Figure 3.5. C_r represents the resonant capacitor and V_{dc} represents the DC-link input voltage after the bridge rectifier in the inverter. R_L and L_r represent the equivalent load resistance and resonant inductance respectively. Q is the main switch and D is the anti-parallel diode.

We should analyze each time period separately and define the initial time of each time period as t=0.

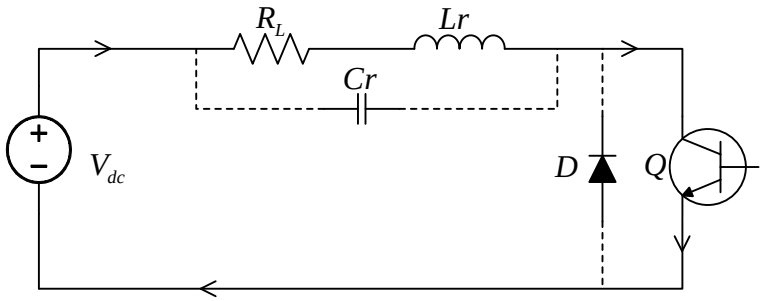

Figure 3.6 [t_0-t_1] Inductor Charging Period

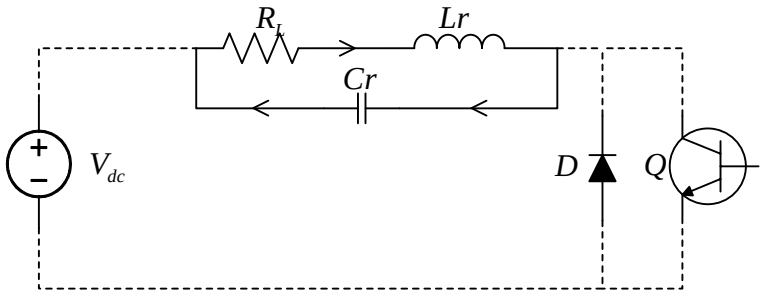

Figure 3.7(a) [t_1-t_2] LC Resonant Stage, Charging Capacitor

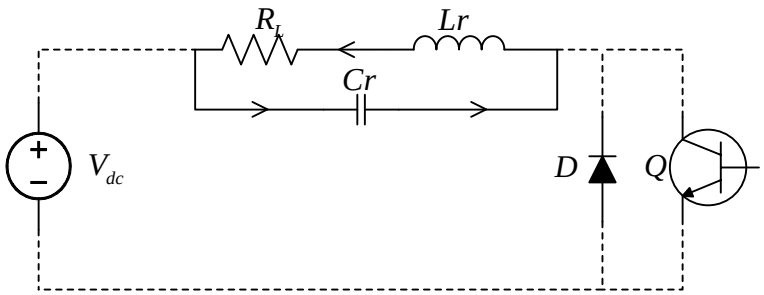

Figure 3.7(b) [t_2-t_3] LC Resonant Stage, Discharging Capacitor

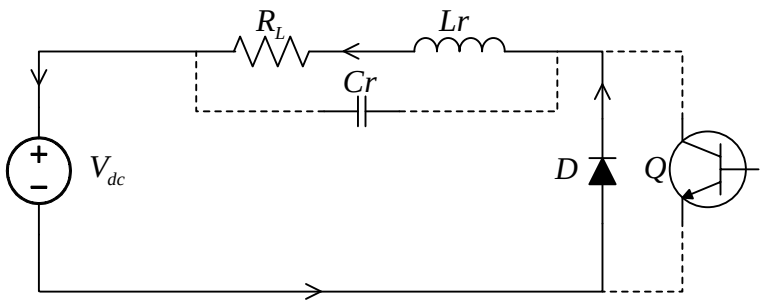

Figure 3.8 [t_3-t_4] Discharging Inductor

(1) [t_0-t_1] Inductor charging period

Consider the inverter is operating in the steady state, and analyze one switching cycle. Define the time right after the main switch turns on, and the current just starts circulating through the switch as t_0. Due to the main switch ZVS turn-on, at t_0, the voltage cross the main switch $V_s = 0$ and $V_c = V_s - V_{dc} = -V_{dc}$. As shown in Figure 3.6, after the main switch Q is turned on, the dc link voltage V_{dc} is now applied across the resonant tank, L_r and R_L in parallel with C_r. Because the voltage across resonant capacitor C_r is already equal to V_{dc}, V_{dc} no longer charges C_r. Current only flows through R_L and L_r . The current flowing through the transistor Q and inductor L_r are equal.

As shown in Fig 3.9 below, i_L increases exponentially. Output power is generated as inductor current flowing through R_L during this period; energy is also stored by L_r. At t_1, i_L reaches maximum value, I_m and the main switch Q turns off. At this time $V_c = -V_{dc}$ and $V_s = 0$. The inductor current i_L changes its direction and starts to flow into resonant capacitor C_r, but the voltage across C_r cannot change its polarity immediately. Therefore, the main switch Q can have zero voltage turn-off.

(2) [t_1, t_2] resonant stage

After the main switch Q turns off, L_r and C_r start to resonate. At the same time, energy is dissipated in R_L, and output power is generated. As the equivalent circuit is shown in Figure 2.10 the resonant period will be divided into two separate stages.

As shown in Fig. 3.9, after the main switch Q turns off, V_c and I_L will decay sinusoidally while voltage across the main switch, V_h, is the summation of V_{dc} and V_c It presents a damped sinusoidal resonance with V_{dc} as center point. Its first positive peak point is the maximum voltage across the main switch. Figure 3-9 shows a more detailed resonant wave during [t_1, t_3] period.

In [t_1, t_2] stage inductor current I_L keeps flowing in positive direction as R_L dissipates power and C_r discharges. When $V_C = 0$, the energy stored inside C_r is released completely. L_r continues to release energy at the same time; part of the energy dissipates in R_L as output power, and the rest of it charges C_r in a sinusoidal fashion. At time t_2, i_L =0 and the energy stored inside L_r is released completely; V_c reaches its maximum value V_{cm}. Thus the voltage across the main switch Q has reached the maximum $V_{hm} = V_{cm}+V_d$.

In the [t_2, t_3] stage as shown in Fig. 3-7, C_r releases energy so i_L starts flowing in reverse direction. Part of the energy dissipates in the R_L as output power; the rest of it is stored inside L_r's magnetic field. Before V_c reach 0V, i_L reaches its negative peak. When Vc =0V the energy stored in C_r is released completely. Then it is time for L_r to start to release its energy in order to keep i_L from flowing in reverse. Part of the energy is dissipated by R_L, while the rest of the energy reversely charges the resonant capacitor C_r.

Since the right side of C_r is clamped by the power source V_{dc}, the right side of C_r's voltage potential continues to decline. When $t = t_3$, $V_c=-V_d$, $V_h = 0V$, diode D starts to conduct; as a result the left side of C_r cannot be decreased further and is clamped at 0V. At this moment, V_c cannot change any more and the charging period ends. However, there is remaining energy in L_r, so i_L is non-zero. Suppose $i_L (t_2) =-I_2$; so there is zero-voltage turn on for the main switch under this condition.

3. $[t_3, t_4]$ Inductor discharging stage

Part of the energy stored inside L is stored in L_R, the rest of it returns to power supply. The absolute magnitude of i_L decays exponentially at t_3, $i_L = 0$, and the energy stored inside L_r is released completely, while the diode naturally block (what voltage?)s . When $V_c =- V_d$, the main switch has been turned on. Excited by the power supply V_d, i_L begins to flow forward again, and repeat the [t0, t1] stage. In fact, when current i_L flows through diode D, there will be a forward voltage drop V_D. While the absolute value of i_L decreases, V_d also decreases.

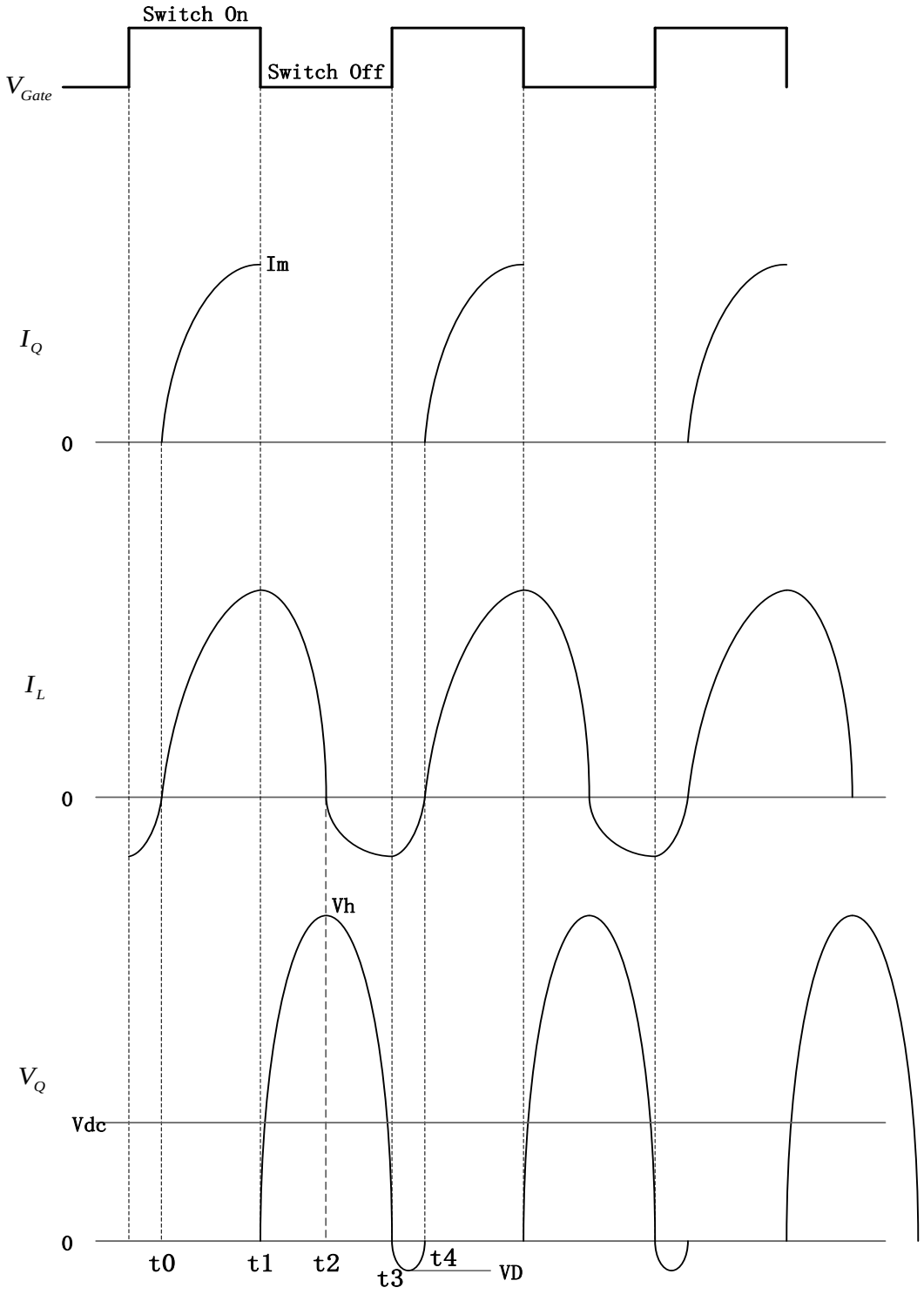

Figure 3.9 Single-Ended Type Inverter Operation Waveform

3.1.4 Single Ended Type ZVS inverter Control Section

Set the main switch's turn-on time as T_{on}, turn-off time as T_{off} As a result, the whole switching cycle period is $T_s = T_{on} + T_{off}$. The main switch's turn on duty cycle is:

$$D = \frac{T_{on}}{T_{off}} \tag{3-1}$$

From the preceding analysis the main switch's turn on time includes the two stage [t_0, t_1]and [t_3, t_4]. In fact, the two phases can be united into one, just extends the time variable t to [t_4, t_1].

As a result of the presence of an inductive discharge period, the main switch turn-on and anti-parallel diode conduction occurs simultaneously. Although the main switch is turned on, no current flows through it. After the [t_3, t_4] period, the diode is natural blocked, and the main switch conducts current. Inductor current I_L starts to increase exponentially from 0A. Note that the main switch's conducting time is T_{on}'; the real duty cycle D' =T_{on} '/T_s. The real duty cycle is smaller than the main switch's driving duty cycle D, resulting in the duty cycle loss. The duty cycle loss is inevitable in this circuit, but will not have a significant impact if this circuit parameter is designed carefully.

The main switch's turn-off moment is controlled by the controller that is used to adjust the input current or power, but the main switch's turn-on moment is decided based on the inverter's resonance parameter and resonance initial conditions. When you change the T_{on}, T_{off} only changes a little bit. Because $T_s = T_{on} + T_{off}$, T_s will change as long as T_{on} changes. Therefore, while changing the duty cycle the switching frequency can also be changed. Thus, the regulation of the cooker is not a pure form of pulse-width

modulation (PWM) or pulse frequency modulation (PFM). It is a combination of PWM and PFM.

Article [1] has made a detailed explanation about the ZVS condition of main switch. This thesis only briefly describes the following control circuit's hardware implementation.

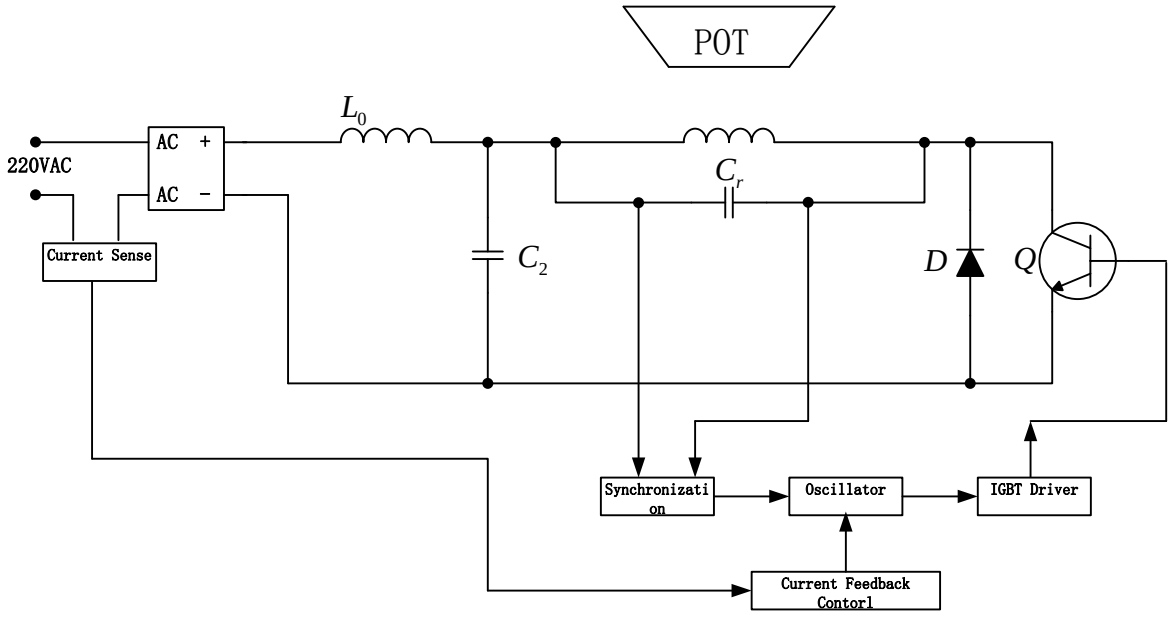

Figure 3.10 Single-Ended Type Inverter Control Section

As shown in Fig. 3.10, the single-ended type inverter usually uses a current transformer to sense the input current and sends the sensed input current information to a microprocessor for power control. In the previous chapter it is explained that when a switching device is turned on, current flows through the inductor to store energy and output power is transferred to the load. When switch turns off, inductance and capacitance will resonate, and output power is generated for the load. The key point is that while device is turned off during the LC resonant time period, there is not any power

dissipation coming from the input power supply. The power dissipation during this period actually comes from the energy stored inside the resonant inductor and resonant capacitor. Based on the circuit analysis, power output can be controlled through the duty cycle. The power can be increased as the duty cycle increases.

Zero-voltage turn-on can easily be achieved by using simple zero-crossing detection as shown in Figure 3.10. As shown in Figure 3.9, shortly after the voltage across the resonant capacitor drops to 0V, the resonant current starts flowing through the switch's anti-parallel diode at t_3, then the device can be turned on under ZVS condition. The ZVS control scheme is an example of self-sustained oscillation, which can generate the turn-on switching signal based on resonant parameters, and can be able to achieve ZVS turn-on load-adaptively.

3.2 The Selection of Power Inverter Topology for Induction Cooking

It is quite interesting to notice that series and parallel resonant inverters have many opposite characteristics.

Parallel resonant inverter does not need an antiparallel diode, while the series resonant inverter requires one. However, parallel resonant inverter needs a series FRED while the series resonant inverter does not require one.

The output current for PRC is square wave, while SRC has sinusoidal output current. The output voltage for PRC is sinusoidal, while SRC has square wave output voltage. The coil current for PRC is inverter current multiplied by the quality factor Q, while the coil current for SRC is just the inverter current.

The peak resonant voltage for SRC is inverter voltage multiplied by the quality factor Q, while the peak resonant voltage current for PRC is just the inverter voltage.

For non-magnetic material induction cooking, because the coil inductance is much larger for aluminum pan than iron pot, resonance will produce excessive resonant voltage on resonant tank.

For both parallel and series resonant inverter the switching device only needs to withstand the voltage drop across the anti-parallel diode. However, for Single Ended type Inverter, the voltage rating for switching device must exceed the resonant voltage across the resonant tank.

Parallel resonant inverter is difficult to control. Series resonant inverter and single ended type inverter are much easier to control.

Based on the previous analysis, the single ended type inverter can be easily controlled by self-sustained oscillation in order to achieve ZVS turn-on load-adaptively. However, for non-magnetic material induction cooking, due to its high quality factor characteristic, there would be a very high resonant voltage stress applied across the resonant element. Today typically high voltage IGBTs can handle up to 1.2kV voltage stress. Therefore, single-ended type inverter topology is unpractical for this type of application. For these reason, a series resonant inverter combined with self-sustained oscillation control is proposed in order to shift the voltage stress from the switching device to the resonant tank while being able to achieve ZVS turn-on load-adaptively.

3.3 Half Bridge Series Resonant Inverter with Self-Oscillation Control Method

3.3.1 Principle of Series Resonant

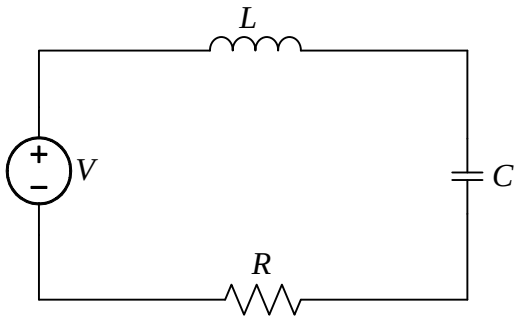

Figure 3.11 Schematic of Series Resonant Circuit

The series resonant circuit was shown in Figure 3.3, inductance L, capacitance C, and the resistor R is connected to create a series circuit. If a voltage source with zero internal resistance was added to this circuit, current I will flow.

The value of the current is:

$$I = \frac{V}{Z} = \frac{V}{R + jX} \tag{3-2}$$

Which Z is the total impedance of the series circuit; X is the total reactance of the series circuit.

$$X = X_L - X_C = \omega L - \frac{1}{\omega C} = \sqrt{\frac{L}{C}}\left(\frac{\omega}{\omega_0} - \frac{\omega_0}{\omega}\right) \tag{3-3}$$

$$\omega_0 = \frac{1}{\sqrt{LC}} \tag{3-4}$$

$$\cos\phi = \frac{R}{Z} = \frac{R}{\sqrt{R^2 + (\omega L - \frac{1}{\omega C})^2}} \tag{3-5}$$

Then the voltage applied across each component is

$$V_R = IR \tag{3-6}$$

$$V_C = \frac{1}{j\omega C} I = \frac{1}{j\omega C} \frac{V}{Z} \tag{3-7}$$

$$V_L = j\omega LI = j\omega L \frac{V}{Z} \tag{3-8}$$

From Eq(3-3), the maximum current I_0 in the circuit was when X=0;

In the case;

$$I_0 = \frac{V}{R_L} \tag{3-9}$$

$$V_R = I_0 R = V \tag{3-10}$$

$$V_{C_0} = \frac{1}{j\omega_0 C} \times \frac{V}{R} = -j \frac{V}{\omega_0 CR} = -jQV \tag{3-11}$$

$$V_{L_0} = j\omega_0 L \frac{V}{R} = jQV = -V_{C_0} \tag{3-12}$$

Where,

$$Q = \frac{\omega_0 L}{R} = \frac{1}{\omega_0 CR} = \frac{1}{R}\sqrt{\frac{L}{C}} \tag{3-13}$$

When $\omega L = \frac{1}{\omega C}$, we have $\omega = \frac{1}{\sqrt{LC}}$, X=0

According to Eq. (3.9-3.12) at resonant frequency, all of the input voltage V is applied across the resistor. Under this condition, the voltage stress on the resonant inductor and resonant capacitor has the same magnitude value but with 180 °of phase shift. The voltage stress's magnitude is Q times the input voltage. Q is called the quality factor of resonant inverter.

The output power can be expressed in Eq. 3-14

$$P = I_o^2 R = \left(\frac{V_1}{|Z|}\right)^2 R \tag{3-14}$$

The output power can be also express in Eq. 3-15

$$P = V_1 I_o \cos\varphi \tag{3-15}$$

Where

I_o: inverter's fundamental output current

V_1: inverter's fundamental output voltage

According to Eq 3.14, the output power can be adjusted by changing the phase between the resonant current and resonant voltage

3.3.2 Operating Principle of Series Resonant Inverter

The schematic diagram of the series resonant inverter, also known as voltage-type inverter, was shown in Figure 3 -1.

The output voltage of the series resonant inverter is approximately a square wave. When the series resonant inverter is operated above resonance, the zero-voltage turn-on switching can occur. With the help of an additional snubber capacitor, the transistor turn-off transitions can also be caused to occur at near zero voltage. This process can lead to significant reduction in the switching losses of IGBTs and diodes.

For the full bridge circuit of Fig. 3.12 the switch output voltage Vs(t) and its fundamental component $Vs_1(t)$, the load current $I_s(t)$ is approximately sinusoidal at a frequency greater than the tank resonant frequency, the input impedance of the tank network $Z_i(s)$ is dominated by the tank inductor impedance. Hence, the tank presents an effective inductive load to the bridge and the switch current $I_s(t)$ lags the switch voltage fundamental component $Vs_1(t)$ as shown in Fig. 3.12. In consequence, the zero crossing of voltage waveform occurs before the current waveform.

For the half cycle $0<t<T_s/2$, the switch voltage Vs(t) is equal to $+V_{dc}$. For $0<t<t_a$, the current $I_s(t)$ is negative and diode D1 conducts. Transistor Q1 conducts when $I_s(t)$ is positive, over the interval $t_a<t<Ts/2$. The waveforms during $Ts/2<t<Ts$ are symmetrical. Since the zero crossing of $V_s(t)$ leads the zero crossing of $I_s(t)$, the transistors conduct after their respective antiparallel diodes. Note that, at any given time during the anti-parallel diode conduction interval $0<t<t_a$, transistor Q1 can be turned on without

incurring switching loss. The circuit naturally causes the transistor turn-on transition to be lossless. In addition, the switching loss associated with reverse recovery of the antiparallel diodes is avoided. Therefore selecting an IGBT with a relatively slow anti-parallel diode is valid. The output capacitances for transistor Q1 and Q2 and diodes D1 and D2 do not result in switching loss.

In general, zero-voltage switching can occur when the resonant tank presents an effective inductive load to the switches; hence the switch zero voltage crossings occur before the zero current crossings. In the bridge configuration, zero-voltage switching is characterized by the half-bridge conduction sequence D1-Q1-D2-Q2, such that the transistors are turned on while their respective antiparallel diodes conduct. Since the transistor voltage is zero during the entire turn on transition, switching loss due to slow turn-on times or due to energy storage in any of the device capacitances does not occur at turn-on.

The transistor turn-off transition in Fig 3.12 is hard switching. In converters that employ IGBTs or other minority-carrier devices, significant switching loss may occur at the turn-off transitions. The current tailing phenomenon causes Q1 to pass through a period of high instantaneous power dissipation, and switching loss occurs.

To assist the transistor turn off process, small capacitors may be added to the legs of the bridge. In a converter employing MOSFETS, the device output capacitances are sufficient for this purpose. A dead time is also introduced into the gate drive signals; so that there is a short commutation interval when both upper and lower transistors are off in order to avoid a short circuit by both upper and lower device turn on. During the normal Q1, D1, Q2, D2 conduction interval the leg capacitor appears in parallel with the

semiconductor switches, and has no effect on the converter operation. However, these capacitors introduce commutation intervals at transistor turn-off. When Q1 is turned off, the tank current $I_s(T_s/2)$ flows through the switch capacitances $C_{snubber}$ instead of Q1 and the voltage across Q1 and $C_{snubber}$ increase. Eventually, the voltage across Q1 reaches Vg; diode D2 then becomes forward-biased. If the MOSFET turn-off time is sufficiently fast, then the MOSFET is switched fully off before the drain voltage rises significantly above zero, and negligible turn-off switching loss is incurred. The energy stored in $C_{snubber}$ is transferred to the tank inductor. The fact that none of the semiconductor device capacitances or stored charges lead to switching loss is the prominent advantage of zero-voltage switching and is the most common motivation for its use. MOSFET converters can typically be operated in this manner, using only the internal drain-to-source capacitances. However, other devices such as IGBTs typically require significant external capacitances to reduce the losses incurred during the IGBT turn-off transition.

Series resonant inverter can be either controlled by external IC-controlled signal or self-oscillation signal generated from the circuit. From the analysis above, we can conclude that while operating frequency is higher than resonant frequency, the voltage across the resonant tank will lead the resonant current and ZVS can be achieved。 In other words, if the voltage across the resonant tank leads the resonant current ZVS can always be achieved. Fig. 3.13 shows the half bridge inverter with self-sustained oscillation control in order for the inverter to achieve ZVS turn-on as resonance changes. The control scheme is explained below.

Suppose the inverter's resonant frequency is in a range from 70 kHz to 130 kHz, which means each resonance cycle is from 14μs to 7.7μs. The DSP chip will trigger a

pulse with duration of 50μs. During this period, the inverter will start to self-oscillate for a few cycles. A LEM current transducer will be used to sense the resonant current and then a high speed comparator will convert the sensed signal into a square wave by using zero crossing detection. Following the zero crossing detection the DSP chip will measure the width of square wave, which is the period of resonance, and use the measured period value as a reference to generate the gate signal before each zero crossing time. As we know, the gate signal is in phase with the resonant voltage; therefore, we can guarantee that the resonant tank voltage will always lead the resonant current and ZVS will be achieved. By Eq. 3-14, the output power can be controlled by adjusting the phase between the resonant current and fundamental resonant voltage. As the gate signal shifts close to zero crossing time, the power will be increased. The opposite is also true, the power will be decreased as the gate signal shifts away from zero crossing time.

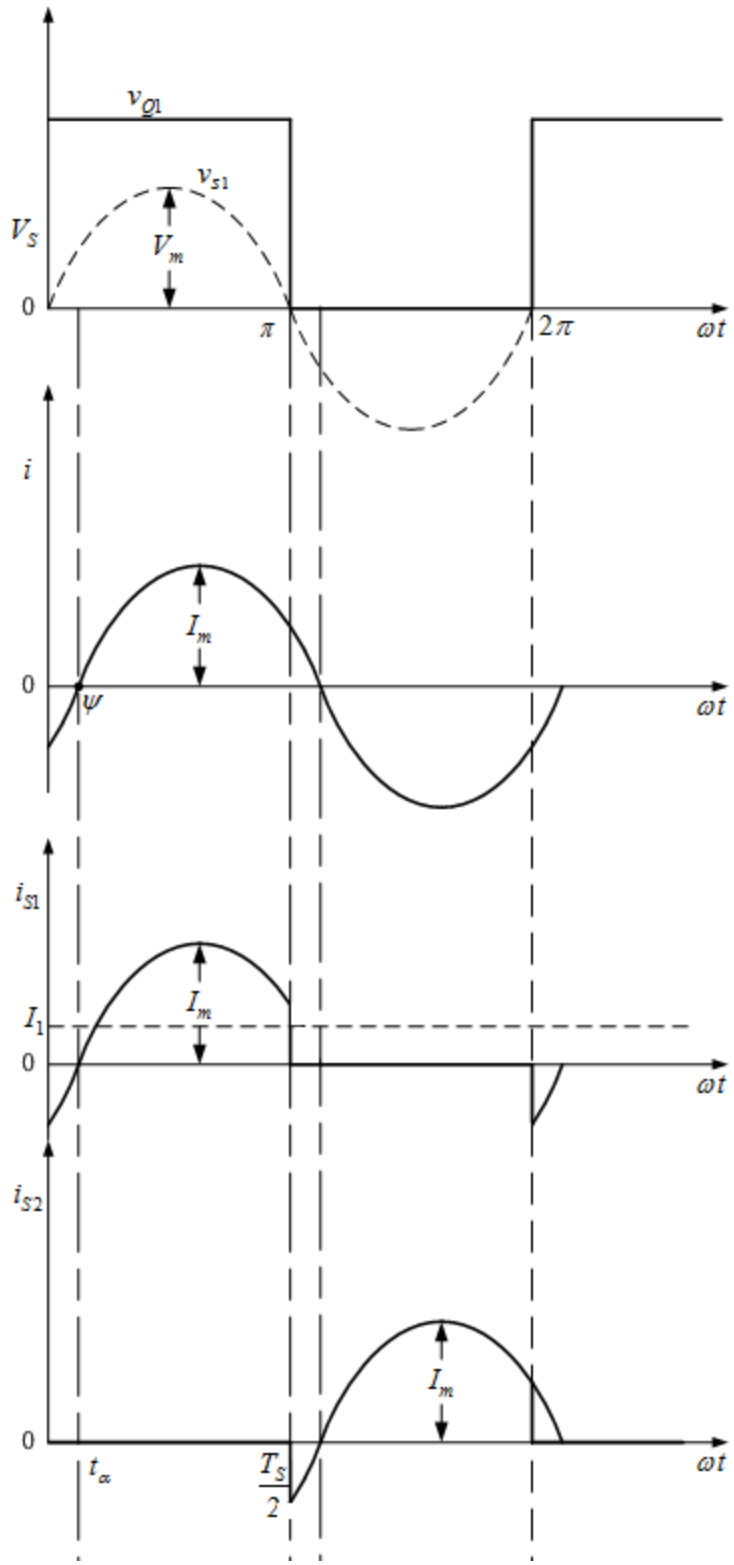

Figure 3.12 Series Resonant Inverter Operation Waveforms

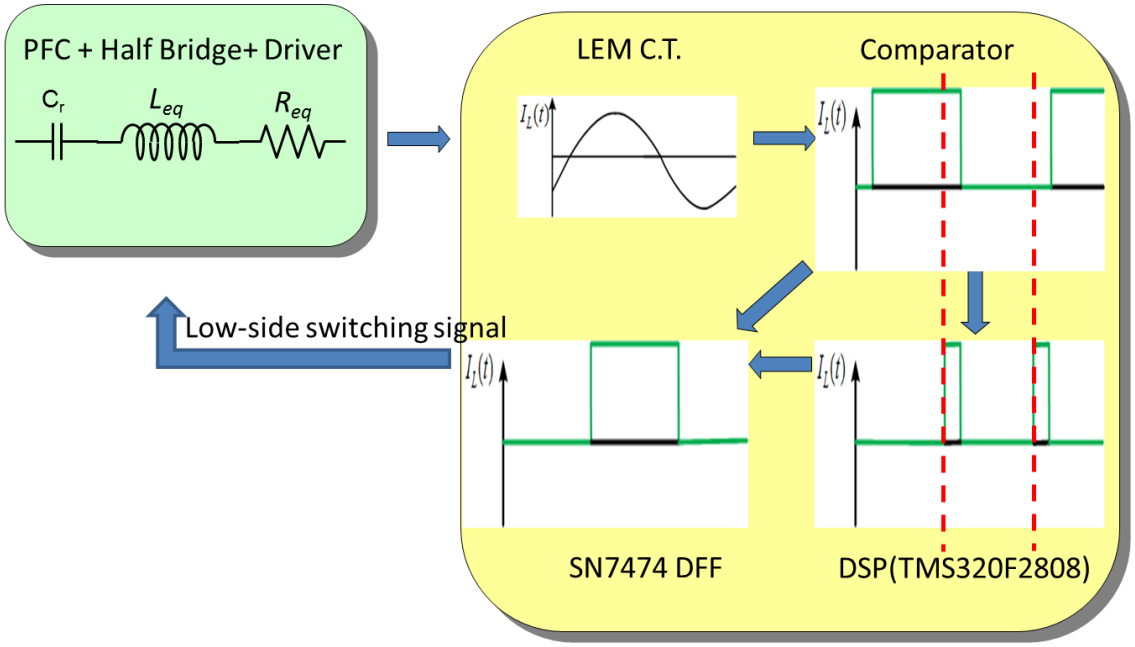

Figure 3.13 Series Resonant Inverter with Self-Sustained Oscillation Control

Chapter 4. Hardware implementation

4.1 Inverter Main Circuit Design

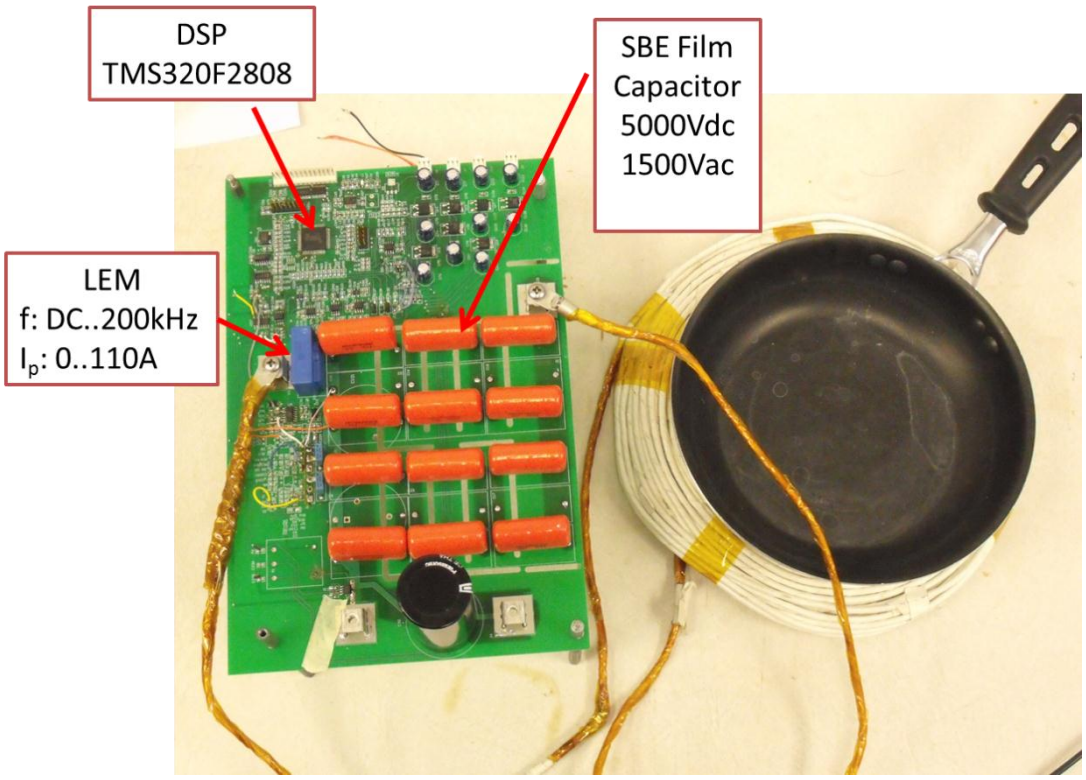

Figure 4.1 Hardware Implementation of 1.8 kW Resonant Inverter

As explained in Chapter 2 for non-magnetic material induction cooking, the induction coil's number of turns and the operating frequency need to be increased to match the iron pan's equivalent resistance. However, the induction coil's number of turns is limited by high resonant voltage stress applied across the resonant elements. In addition, the operating frequency is limited by switching loss.

The induction coil used in this project is shown in Fig. 2.8 is 1.126mH with N=96 turns and based on the experiment, while the cooking pan is placed on top of the induction coil, its equivalent inductance would fall into the range of 690 μH -457 μH. The resonant frequency is limited to be 100 kHz, which is the maximum operation

frequency most semiconductor device such as IGBT and MOSFET can handle. In this project the resonant frequency is set around 80kHz for an acceptable safe margin. Therefore, the resonant capacitor's value will be 7.5nF. Suppose the cooking pan's surface resistance is approximate 3Ω. By Eq. 3-13, the quality factor is obtained

$$Q = \frac{1}{R}\sqrt{\frac{L}{C}} = \frac{1}{3\Omega}\sqrt{\frac{575\mu H}{7.5nF}} = 92.3$$

.

Therefore, this is a high quality factor system and the selected resonant capacitor must be able to handle high voltage stress. In this project SBE 719P series capacitor is chosen due to its high voltage capability and low ESR at high frequency. The capacitor has 1.5 kV AC voltage rating and 5 kV DC voltage rating. But nevertheless, the capacitors are still needed to be connected in series for the extreme large voltage stress (may up to 15kV) applied on them caused by the high quality factor system. In addition, the induction coil is constructed by Litz wire, which is also pre-wrapped by electrical insulated tape, to prevent the electric arc caused by the large voltage stress as shown in Figure 2.9.

IGBT is chosen over MOSFET due to its low conduction loss at high breakdown voltage. The maximum voltage applied on the switching device is inverter's DC-link input voltage. Taking into account the surge voltage switching and practical safety margin, general we choose IGBT with 1.5 times DC-link voltage rating, therefore if DC-link voltage is 400V, the preferred IGBT voltage rating is 600V.

Assume the cooking pan's equivalent resistance R_{eq} is 3Ω, then inverter's fundamental output current at the maximum power P=1800W is

$$\mathrm{I} = \sqrt{\frac{\mathrm{P}}{R}} = \sqrt{\frac{1800W}{3\Omega}} = 24.5A$$

$$\mathrm{I}_{peak} = \sqrt{2}I = 34.65A$$

Based on the above calculation IGBT can be selected. As a result of the inverter operating in ZVS turn-on condition, the turn-on switching loss and diode reverse recovery loss is negligible. The turn-off loss is significantly reduced by external lossless capacitor. If only considering the conducting loss, IGBT can be selected in accordance with the datasheet's given V_{ce} vs I_c chart as shown in Fig. 4.2, with a Fairchild IGBT HGTG20N60A4D is selected. [12]

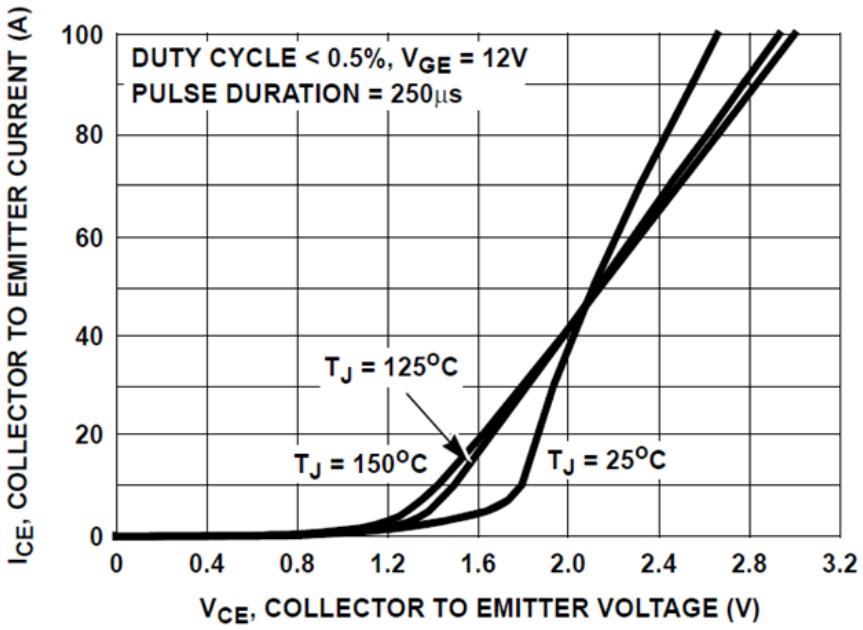

Figure 4.2 Collector-to-emitter Current vs. Collector-to-emitter On-State Voltage

4.2 Inverter Control Circuit Design

Current sensing is a crucial part in this design because the inverter relies on fast and accurate current sensing information for frequency tracking control. In the design,

the current sensor is required to accurately sense the resonant current operating up to100 kHz with peak amplitude of 34.65A. Therefore, common current transformer is not appropriate because they usually can only handle a few amperes current and low frequency (up to 20kHz). Thus, LEM 50-P current transducer, a hall-effect transducer is chosen as shown in Fig. 4.3. Its primary current measure range is 0-110A and frequency bandwidth is 0-200kHz

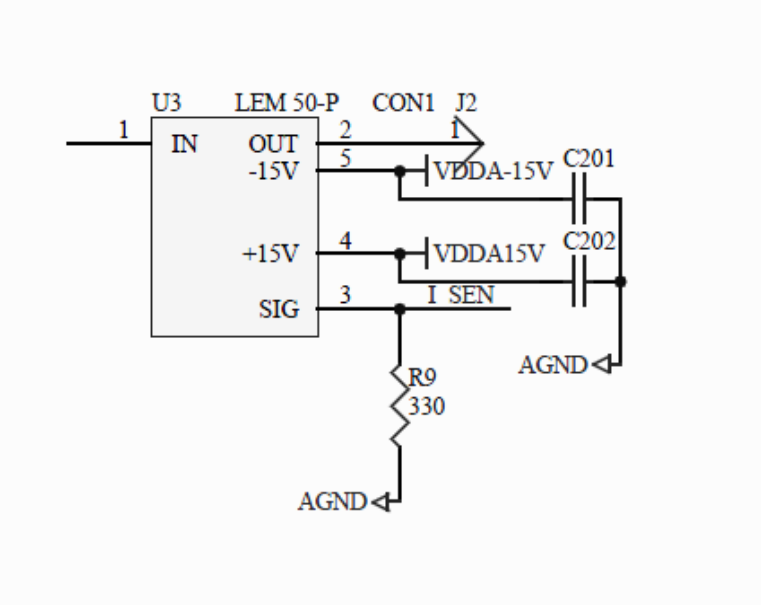

Figure 4.3 LEM Current Sensor

The circuit to generate a self-sustained oscillation trigger pulse is shown in Figure 4.4. By controlling SN74LS74A D-flip flop's CLEAR and PRESET pin using DSP, a trigger pulse can be generated with a time duration programmed by DSP. . Firgure 4.5 shows SN74LS74A D-Flip Flop's function table. Suppose initially PRE is High and CLR is Low, then OUTPUT Q is Low. To start generating a self-sustained oscillation trigger pulse, PRE is changed to Low and CLR is changed to High, then OUTPUT Q changes to High, sending a trigger pulse into the gate driver and creating a self-sustained

oscillation in the inverter circuit. After a short period, both PRE and CLE will set to High, indicate the beginning of self-oscillation controlled by CLE pin. In this design, the pulse duration is set to be 50μs. During this period, the inverter will start to self-oscillate for a few cycles and the LEM current transducer will sense the resonant current as shown in Fig. 4-3.

The sensed current would be converted into a square waveform by a zero crossing detection circuit, which uses a high frequency comparator TLV3501as shown in Fig. 4.6. Following by the zero cross detection; DSP chip will measure the width of square wave, which is the period of resonance, and use the measured period value as a reference to generate the gate signal for the next resonant cycle so in this way the upper device will be always turned on during negative resonant cycle and the lower device will always be turned on during the positive resonant cycle. And ZVS turned on is achieved no matter what the resonant frequency be because the resonant frequency is tracked and sensed in real-time.

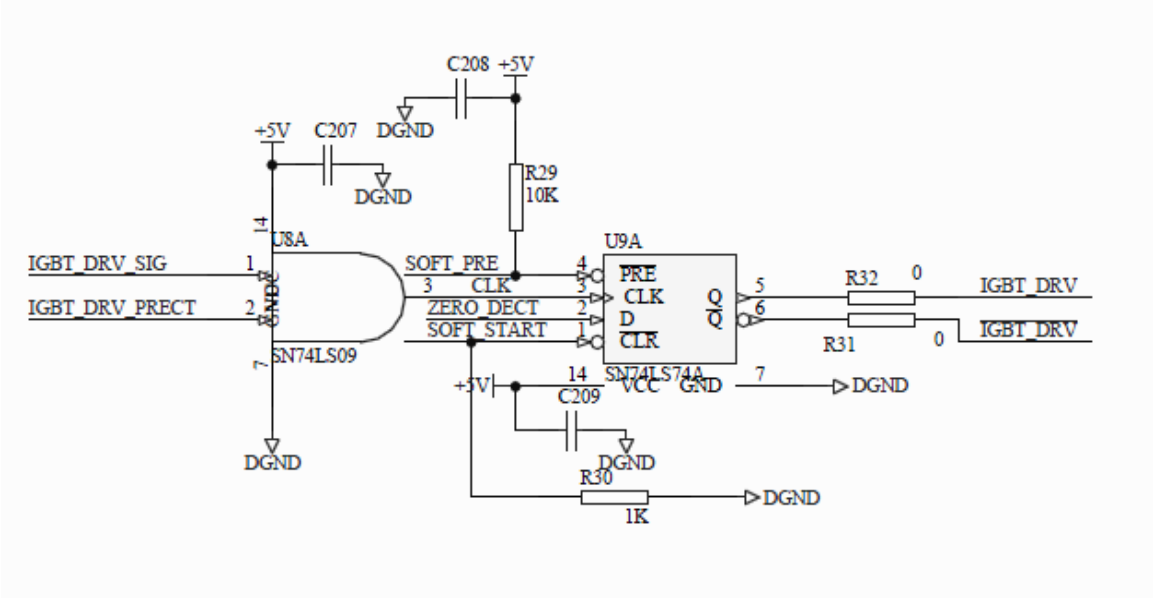

Figure 4.4 SN74LS74A D-Flip Flop for Self-Sustained Oscillation Trigger Pulse

FUNCTION TABLE

INPUTS				OUTPUTS	
$\overline{PRE}$	$\overline{CLR}$	CLK	D	Q	$\overline{Q}$
L	H	X	X	H	L
H	L	X	X	L	H
L	L	X	X	H	H
H	H	↑	H	H	L
H	H	↑	L	L	H
H	H	L	X	Q_0	$\overline{Q}_0$

Figure 4.5 SN74LS74A D-Flip Flop Function Table

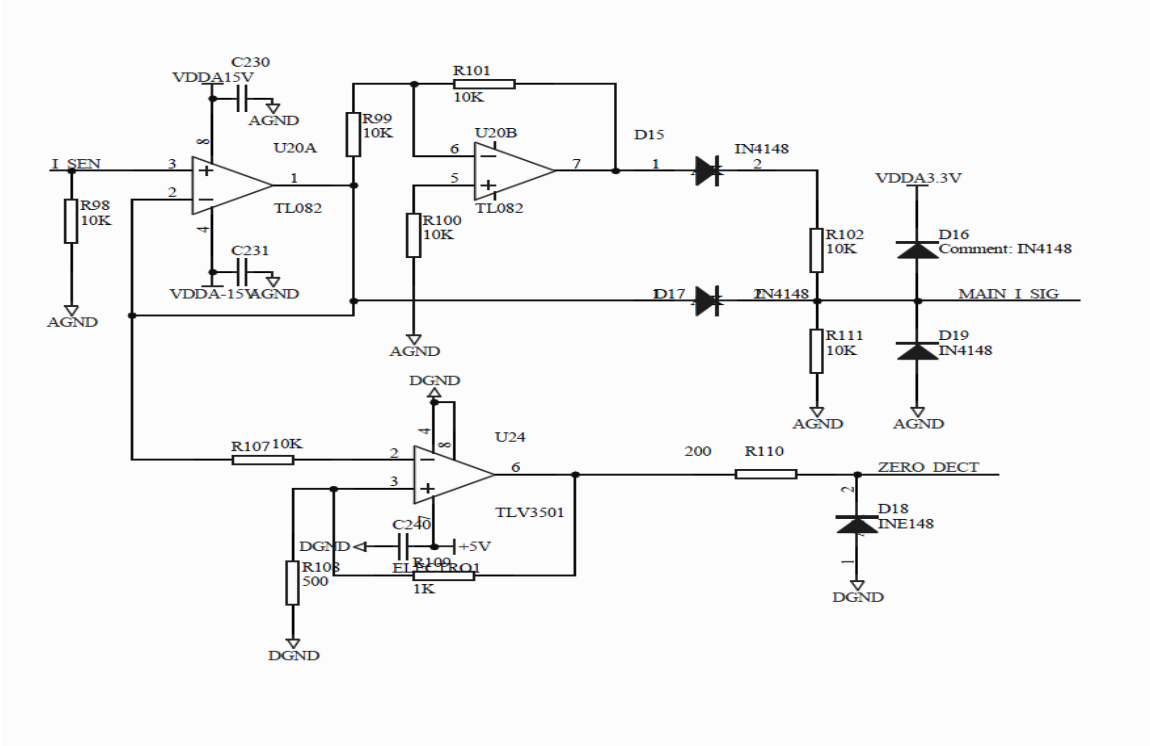

Figure 4.6 TLV3501 High Frequency Comparator for Zero-Crossing Detection Voltage

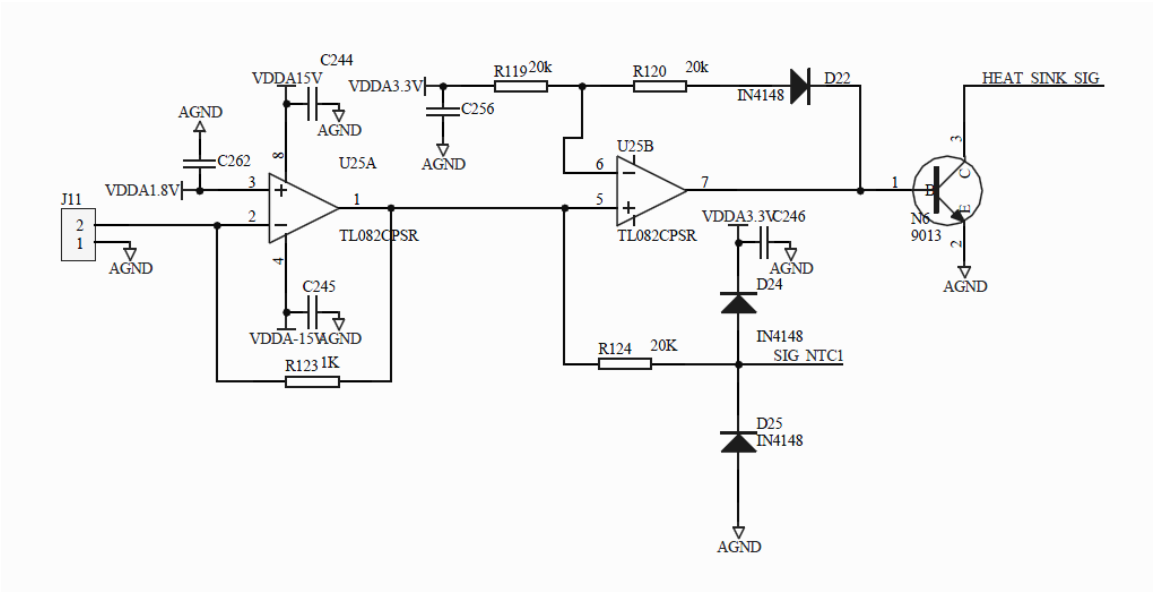

Figure 4.7 Over-voltage, Over-current, and Over-temperature Protection Circuit

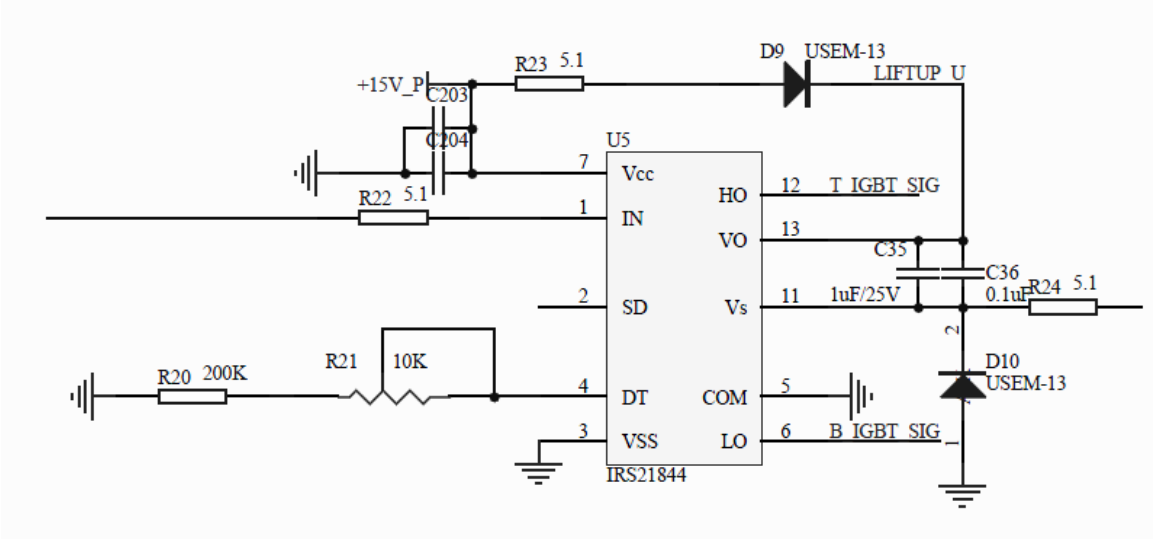

Figure 4.8 IRS21844 Bridge Driver IC

2.5.1 Half bridge IGBT Driver

Driver circuit can be divided into two categories: a commercial driver IC which integrate everything inside it or customized driver circuit constructed by discrete components

Obviously, a customized driver circuit involves with many discrete components, no need to say the difficulty to calculate and choose component parameters. Driver circuit with additional protection features is even more complex, therefore, such kind of driver circuit usually is only applicable to drive small power device. For high power application, integrated driver IC is used while taking the consideration of improving driver circuit's anti-interference ability, simplifying circuit design, and reducing unit volume.

In the design, the driver IC requires a programmable dead time function. Due to IGBT's high input impedance characteristic, it requires very simple drive capability. In this project, bridge driver IRS21844 is chosen with charge-pump functionality for high side device and 600V/20A driving capability as shown in Fig. 4.8.

3.4.4 Overvoltage, overcurrent, and over temperature protection circuit

Overcurrent and overvoltage protection circuit are shown in Figure 4.7. Over current protection circuit monitors the inverter's input current and resonant current. Once an over-current is detected, it will send a signal to DSP and shut down the device immediately in order to prevent permanent damage to the device. Over-temperature protection circuit monitors the heat sink temperature, induction coil temperature by using a NTC thermal resistor. When exceeding the reference temperature, output low voltage, and DSP may know there is over temperature that has occurred and would shut down the induction cooker or reduce the power accordingly.

4.3 Testing Results and Control Strategy Study

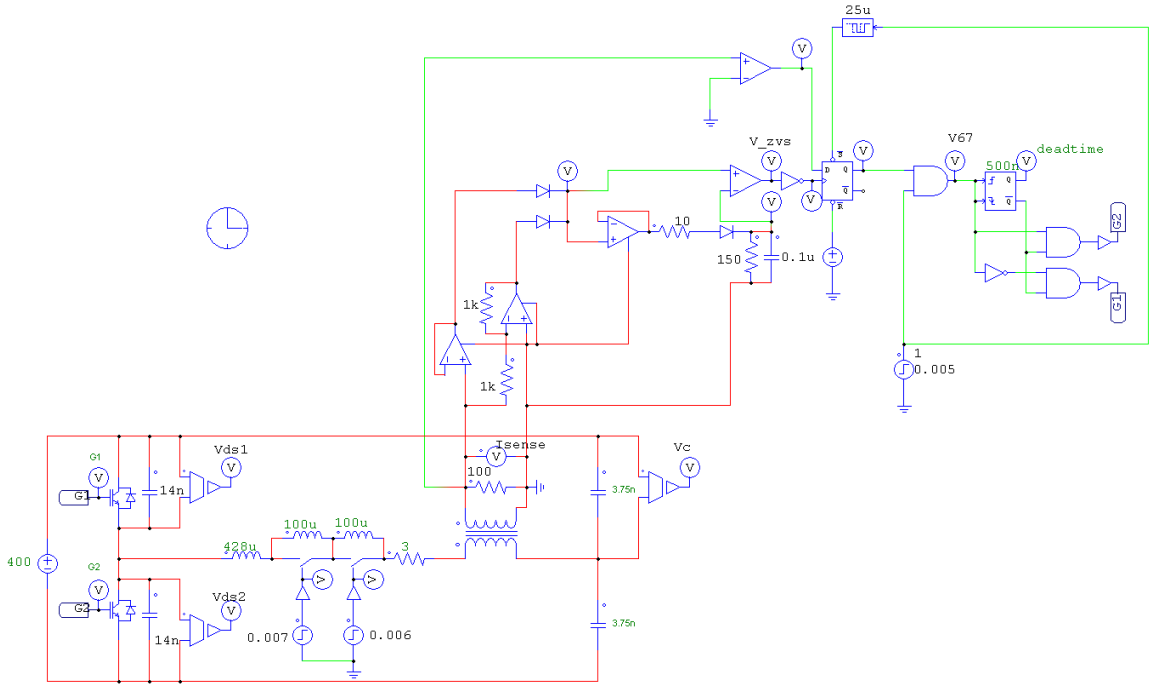

Figure 4.9 Simulation of Half-Bridge Inverter with Frequency Adaptive Control

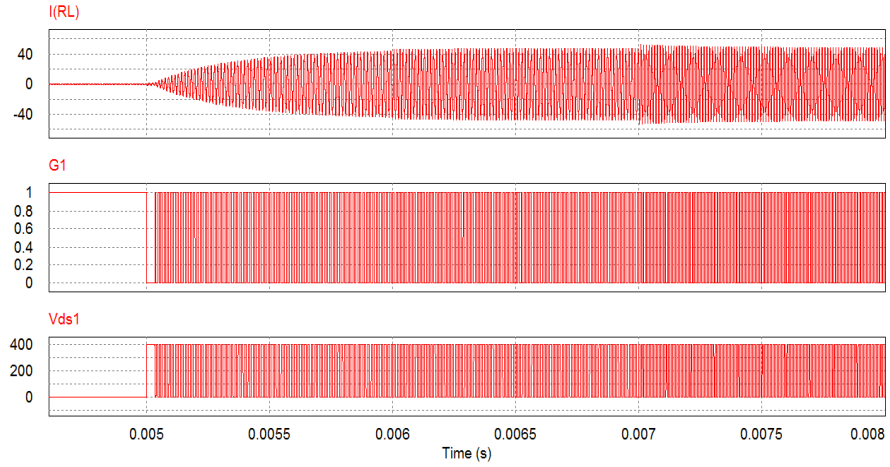

Figure 4.10 Simulation Result of Half-Bridge Inverter with Frequency Adaptive Control

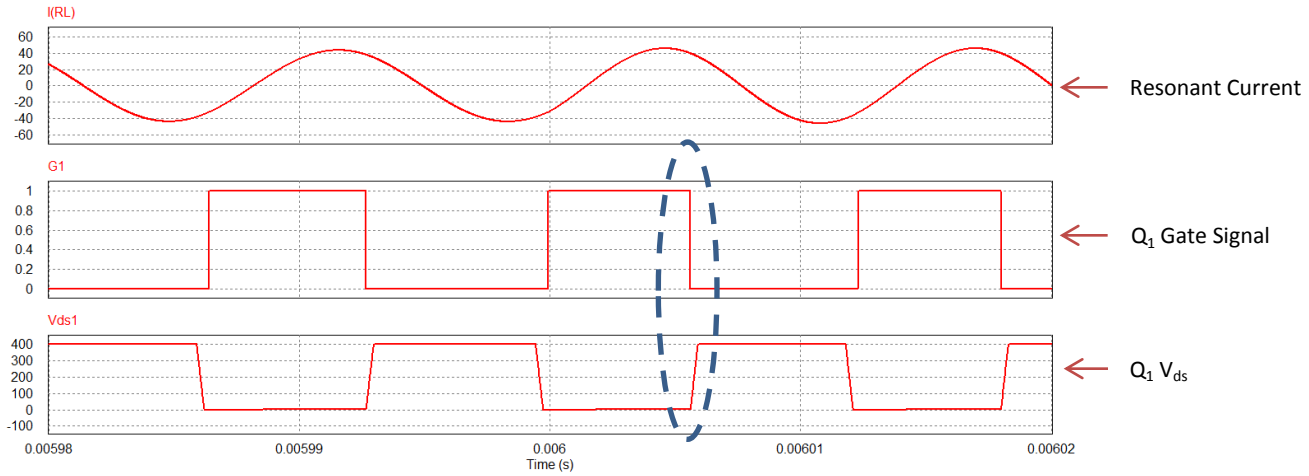

Figure 4.11Simulation Result of Half-Bridge Inverter with Frequency Adaptive Control at 0.006second with resonant frequency changes from 88.89 kHz to 80kHz

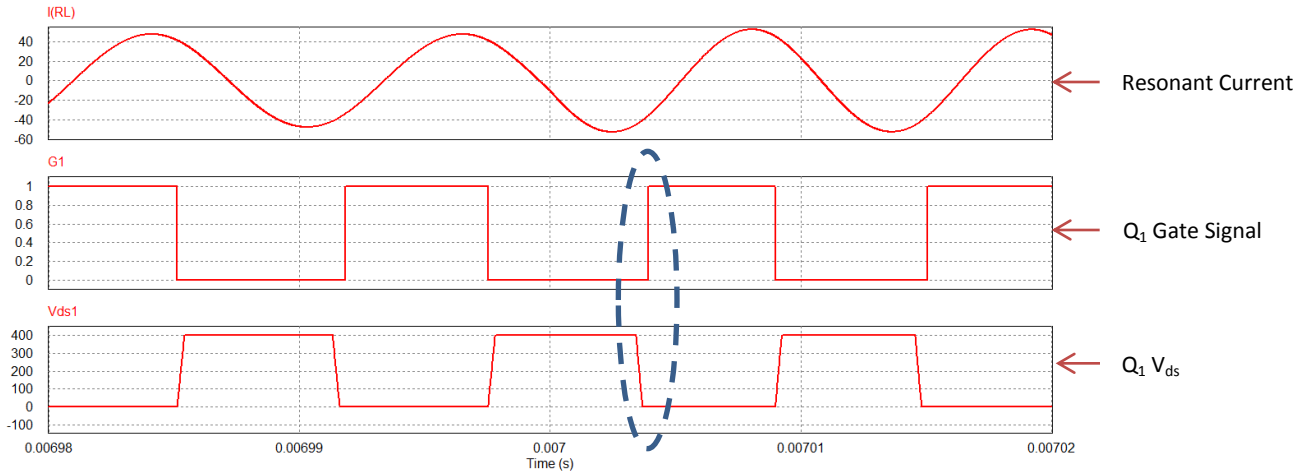

Figure 4.12 Simulation Result of Half-Bridge Inverter with Frequency Adaptive Control at 0.007second with resonant frequency changes from 80 kHz to 73.37kHz

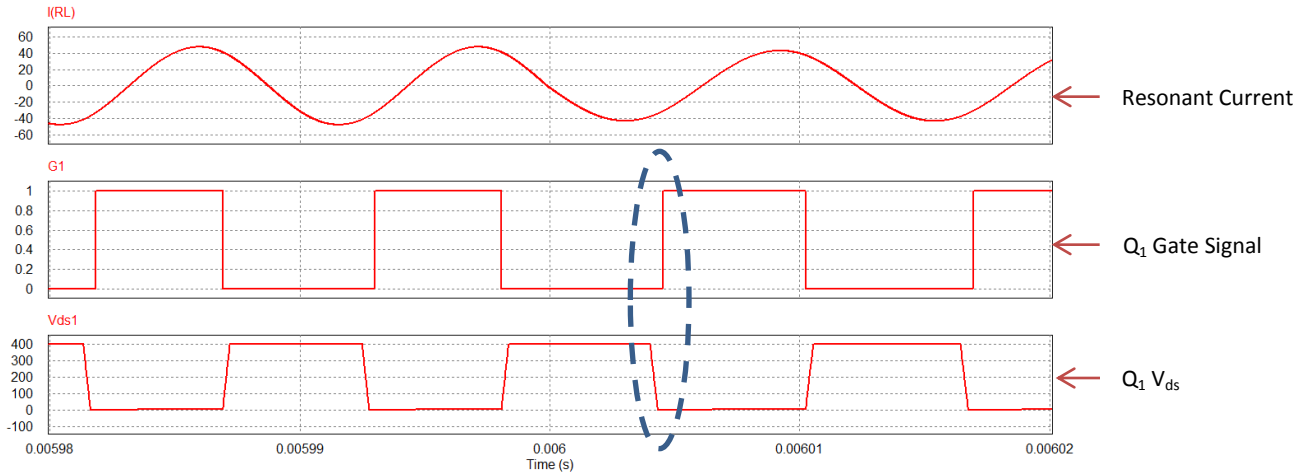

Figure 4.13 Simulation Result of Half-Bridge Inverter with Frequency Adaptive Control at 0.006second with resonant frequency changes from 73.37kHz to 80kHz

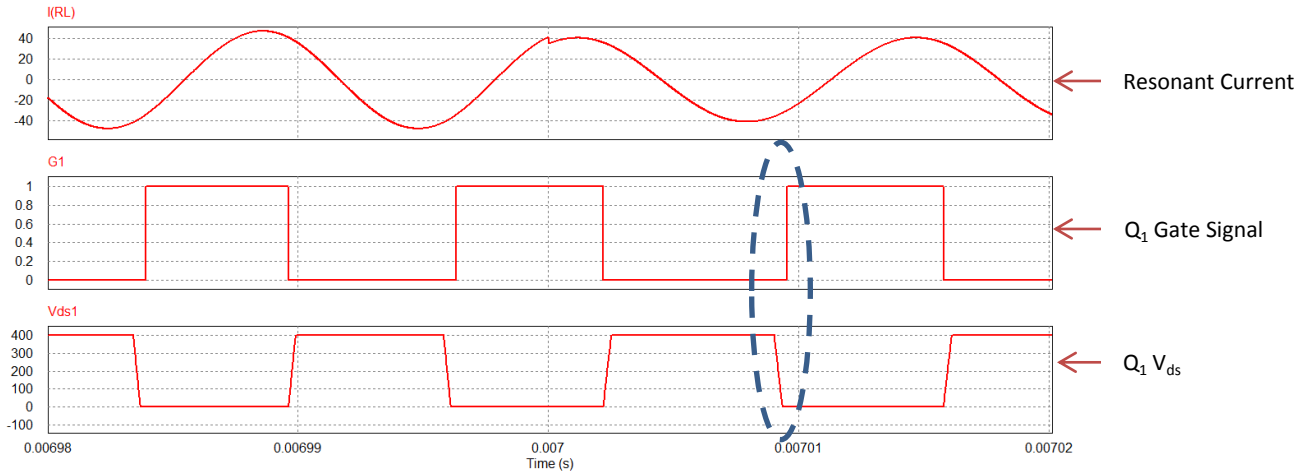

Figure 4.14 Simulation Result of Half-Bridge Inverter with Frequency Adaptive Control at 0.007second with resonant frequency changes from 80 kHz to 88.89kHz

Fig. 4.10 shows a Psim simulation circuit of half-bridge resonant inverter with self-oscillation control. The load resistor is set to be 3Ω, which is aluminum pan's typical effective resistance according to our experimental results. The resonant capacitor is 7.5nF and resonant inductor is set to be 428μH initially. In order to verify our theory, at 0.006 second, the resonant inductor changes its value to 528μH, and reduces its resonant frequency from 88.88 kHz to 80 kHz. Again at 0.007 second, the resonant inductor changes its value to 628μH, lowering its resonant frequency to 73.37 kHz.

As shown in Figure 4.11-4.12, at t=0.006s and t=0.007s, although the resonant frequency changes immediately, the switching frequency can also be adaptive to the new frequency while keep the phase between resonant voltage and resonant current fixed, and keep producing the same output power. Figure 4.13-4.14 have similar simulation results while the resonant frequency suddenly increases from 73.37kHz to 80kHz, then to 88.88kHz.

Following the simulation results, a prototype of 1.5kW high frequency inverter with self-sustained oscillation control was built and test results further verify our control theory and simulation result. Figure 4.15-4.18 show the induction cooker prototype can be able to track the resonant frequency and maintain ZVS turn-on as resonant frequency changes. During the test, a pan is shifted horizontally without losing touch with the cooker's ceramic surface. As the pan shifts, the coupling between the induction coil and the pan changes, leads to the change of resonant inductance and resonant frequency. As shown in Figure 4.21-4.24, the device is always turned on under ZVS condition and the induction cooker operates very reliable without any device damage.

In addition, several power control method are tested and discuss. By comparing different power control method and selecting the appreciate one, we want to improve the system reliability and even push the output power higher beyond 1.5kW. The ultimate goal is to be able run the induction cooker unit at 2.5 kW.

Usually an induction cooker consists with a high frequency inverter and a front-end PFC circuit. Combining with the front end PFC circuit gives us more flexibility in term of control strategy. The first control strategy is the combination of boost-type PFC circuit and a high frequency circuit with phase shift control. In this case the input voltage is fixed at 400V for universal household power supply. The output power can be controlled by adjusting the phase shift between resonant current and resonant voltage by Eq. 3-15. The control scheme is very straightforward. However, as explained in previous chapter, since non-magnetic material's effective resistance is too small, just 3Ω in this design. By Eq. 3.24, at resonant frequency, all dc-link voltage is applied on the load resistor, leads to high output power and ultra-high voltage stress on the resonant elements.

$$\mathrm{P} = \frac{V^2}{R} = \frac{400^2}{3\Omega} = 53kW$$

Therefore, in order to avoid making too much output power and damage our devices, the switching frequency must be shifted away from the resonant frequency to create a phase shift between the resonant voltage and current. The drawback is that the transistor is turned off at relative high current, results in very large turn off switching loss. Figure 4.15-4.17 show Psim's simulation results for phase shift power control strategy. The input voltage is fixed at 176V and the resonant frequency is 78.6 kHz. As the phase

shift between the resonant voltage and resonant current decrease and the switching frequency moves toward the resonant frequency, the output power increase according to Figure 4.15-4.17. The simulation results are verified by hardware measurement using prototype board with same configuration. The hardware testing result are shown in Figure 4.25-4.27.

Another way to control the output power is by adjusting the DC-bus voltage while keep the switching frequency very close to resonant frequency. In this way, the inverter can achieve ZVS turn on and at the turn off moment, since the resonate current has already dropped to near zero ampere; the turn off switching loss can be reduced significantly. Same issue here is that DC link voltage can not be very high; otherwise, the output power will be too large. In addition, a varying dc link voltage source is difficult to implement because most PFC circuit produces a fixed dc-link voltage. Figure 4.18-4.20 show Psim's simulation results for dc-bus voltage power control strategy. The phase shift between the resonant voltage and resonant current is fixed and the switching frequency is fixed at 78.98 kHz, which is very close to the resonant frequency. As explained, the input voltage must be a small value. In this case, the input voltage changes from 92V for 300W output power to 172V for 900W output power and the switching frequency moves toward the resonant frequency. The simulation results are verified by hardware measurement using prototype board with same configuration. The hardware testing result are shown in Figure 4.28-4.30.

The comparison of those two control strategy are listed below in Table 4.1 and 4.2. as we can see, at about same power, by implementing the dc-link voltage control and let

switching frequency close to resonant frequency, the device temperature is significant lower than phase-shift control.

V_{in}	P_{in}	F_{req}	I_{pk-pk}	T_{IGBT}	$T_{heatsink}$	$T_{capacitor}$
151V	300W	79.4 kHz	27.6A	39.6	31.9	35.4
151V	500W	79.2 kHz	35.1A	42.5	33.4	37.1
151V	920W	78.8 kHz	49.5A	47.5	36.9	43.1

Table 4.1 Testing Result for high frequency inverter with phase shift control

V_{in}	P_{in}	F_{req}	I_{pk-pk}	T_{IGBT}	$T_{heatsink}$	$T_{capacitor}$
82V	290W	78.8 kHz	28.1A	36.3	28.7	34.9
108V	500W	79.1 kHz	35.6A	39.3	31.7	36.8
145V	890W	79.2 kHz	48.6A	44.4	34.4	41.5

Table 4.2 Testing Result for high frequency inverter with DC-bus voltage control

Figure 4.31 show the last option, which is triple resonant frequency output power controlled. The output power is still control by the phase shift between resonant current and resonant voltage. The only difference is this time for each switching cycle, the inverter will oscillate three times and the switching loss will also be reduce dramatically to 1/3. The drawback is that the output power also reduces to 1/3 at the same input voltage condition. As shown in Figure 4.31, in order to generate enough power, the DC-bus voltage must be increased to a considerable high value, in this case, 406.7V. It also creates a very high resonant current, in this case, 32.7A peak current. The high resonat current may give trouble for device selection.

Figure 4.28 shows the comparison of different control strategy. As explained, the phase shift control would experience high turn-off loss since the device is turned off at high current condition. The triple frequency control dramatically reduces the switching loss by 2/3. However, it is still phase-shift control and device still turns off at high

current level. As Fig. 4.10, 4.11, 4.12 shown, while the inverter operates close to resonant frequency, its switching loss is lowest. Therefore, for future research, it is worth to use the combination of fundamental, triple frequency for power control while keep the switching close to resonant frequency.

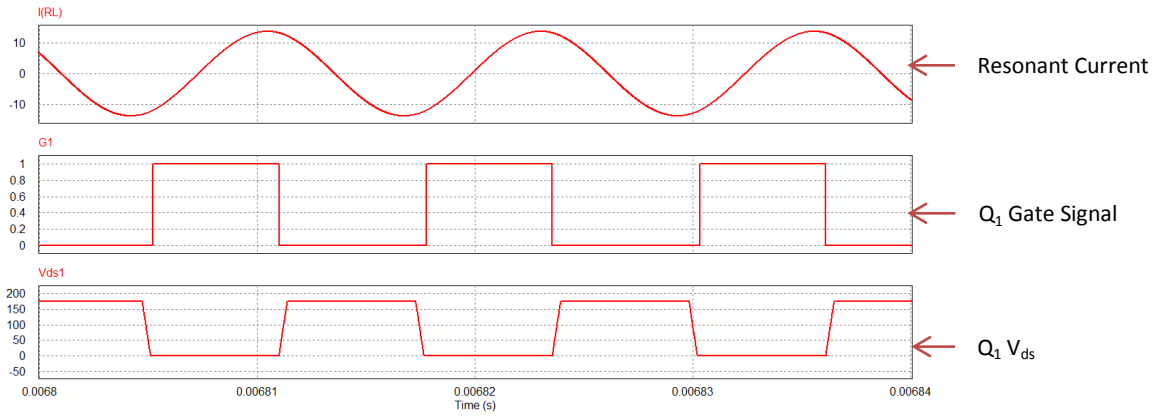

Figure 4.15 Simulation Result of Half-Bridge Inverter with Frequency Adaptive Control, ZVS Turn-on at 300W, f=79.68kHz, Vin=176V, Ipk=13.76A for Phase Shift Power Control Test

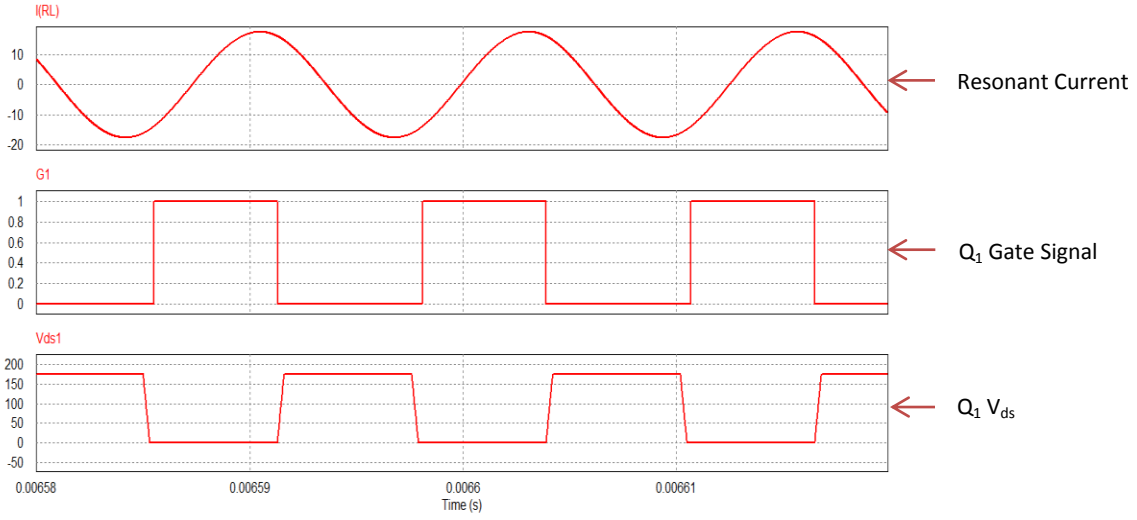

Figure 4.16 Simulation Result of Half-Bridge Inverter with Frequency Adaptive Control, ZVS Turn-on at 500W, f=79.365kHz, Vin=176V, Ipk=17.78A for Phase Shift Power Control Test

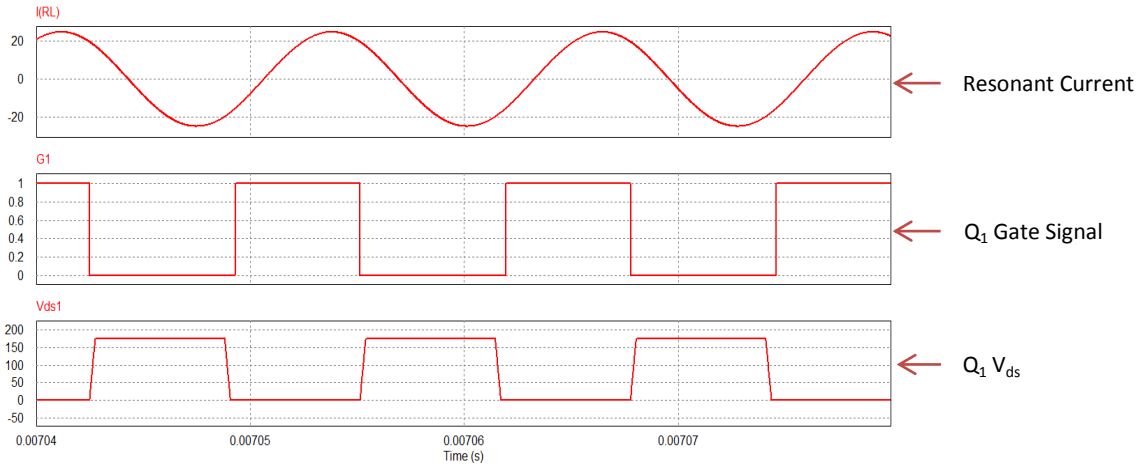

Figure 4.17 Simulation Result of Half-Bridge Inverter with Frequency Adaptive Control, ZVS Turn-on at 920W, f=79.11kHz, Vin=176V, Ipk=24.7A for Phase Shift Power Control Test

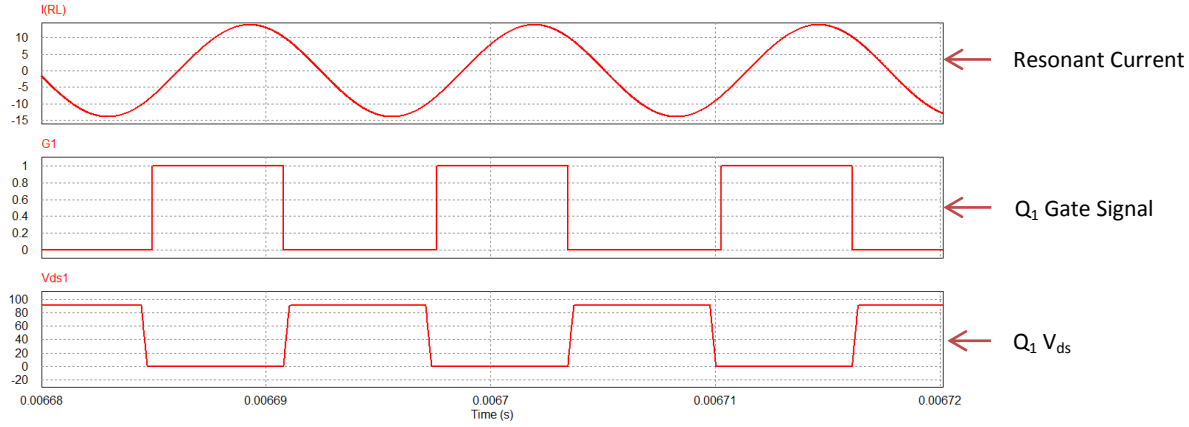

Figure 4.18 Simulation Result of Half-Bridge Inverter with Frequency Adaptive Control, ZVS Turn-on at 290W, f=78.98kHz , V=92V, Ipk=14.09A for dc voltage control

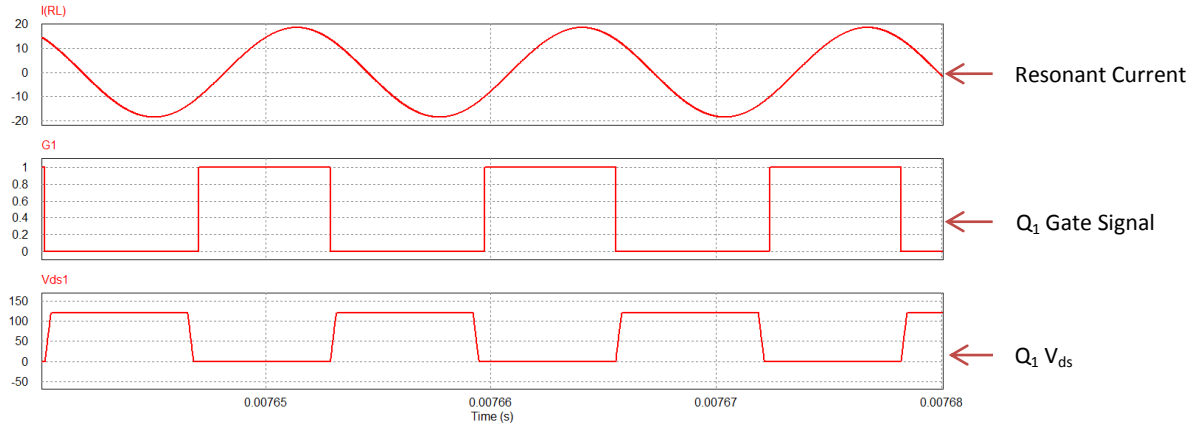

Figure 4.19 Simulation Result of Half-Bridge Inverter with Frequency Adaptive Control, ZVS Turn-on at 500W, f=78.98kHz , V=121V, Ipk=18.532A for dc voltage control

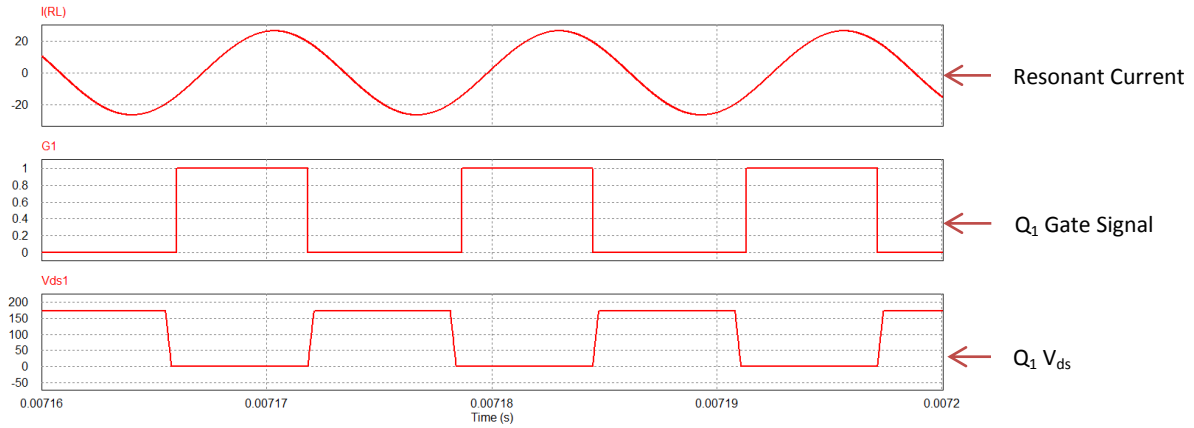

Figure 4.20 Simulation Result of Half-Bridge Inverter with Frequency Adaptive Control, ZVS Turn-on at 890W, f=78.98kHz , V=172V, Ipk=26.344A for dc voltage control

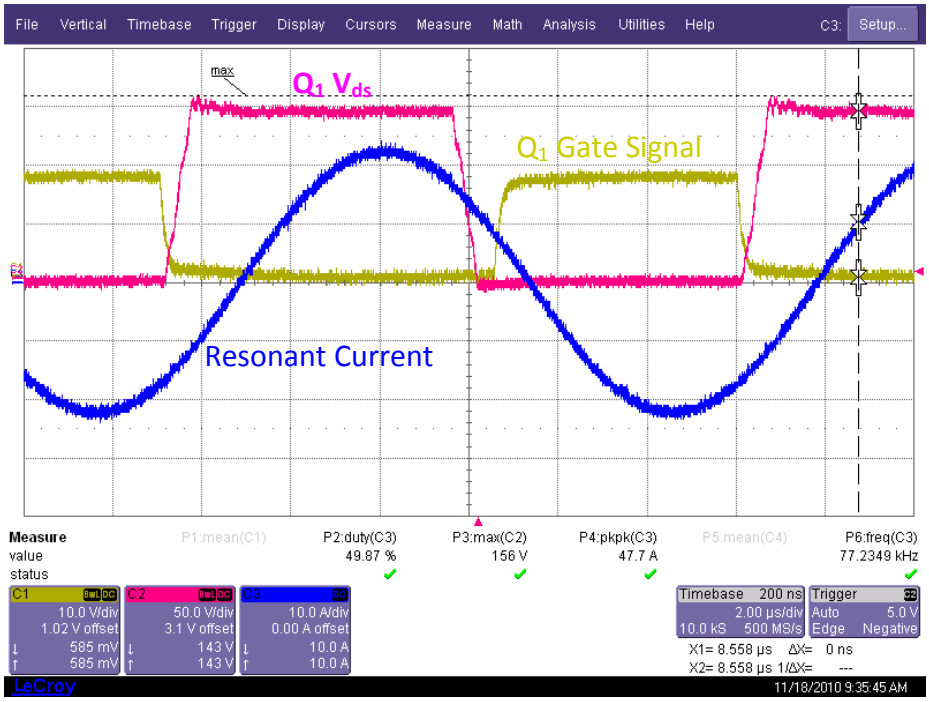

Figure 4.21 ZVS Turn-on at f=77.23 kHz for Frequency Tracking Test

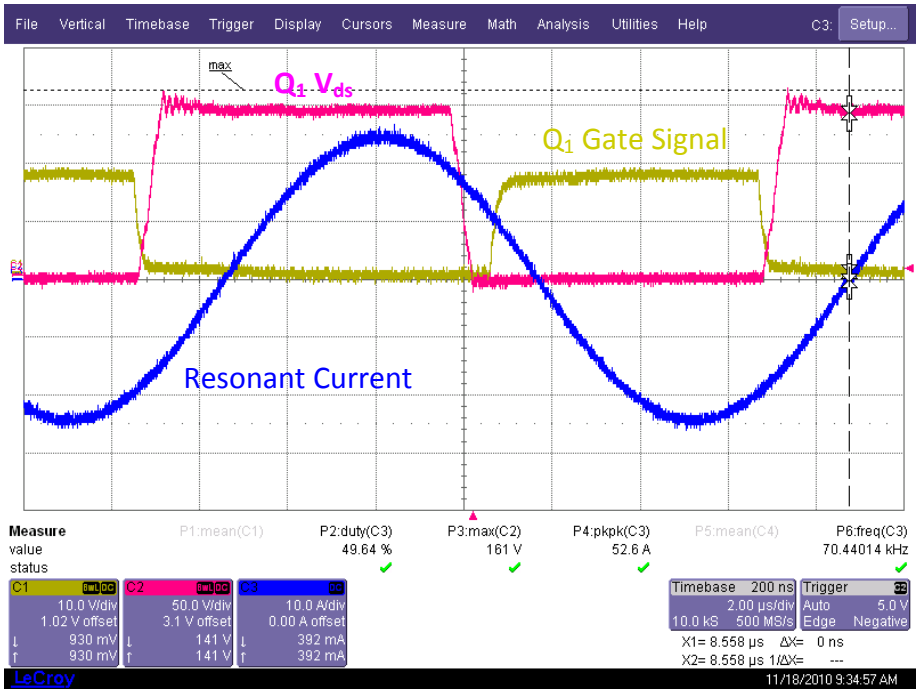

Figure 4.22 ZVS Turn-on at f=70.44 kHz for Frequency Tracking Test

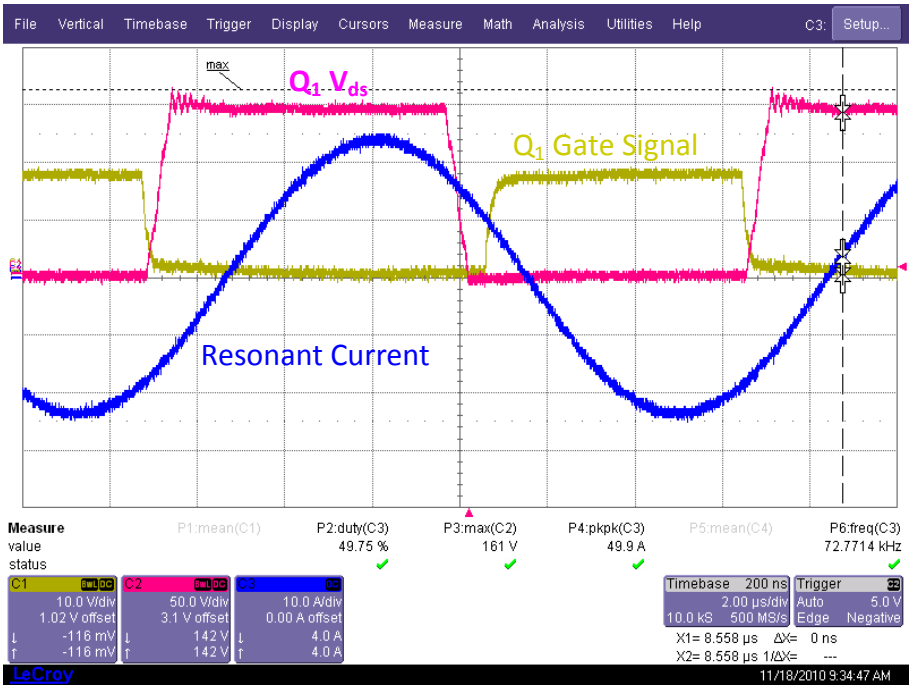

Figure 4.23 ZVS Turn-on at f=72.77 kHz for Frequency Tracking Test

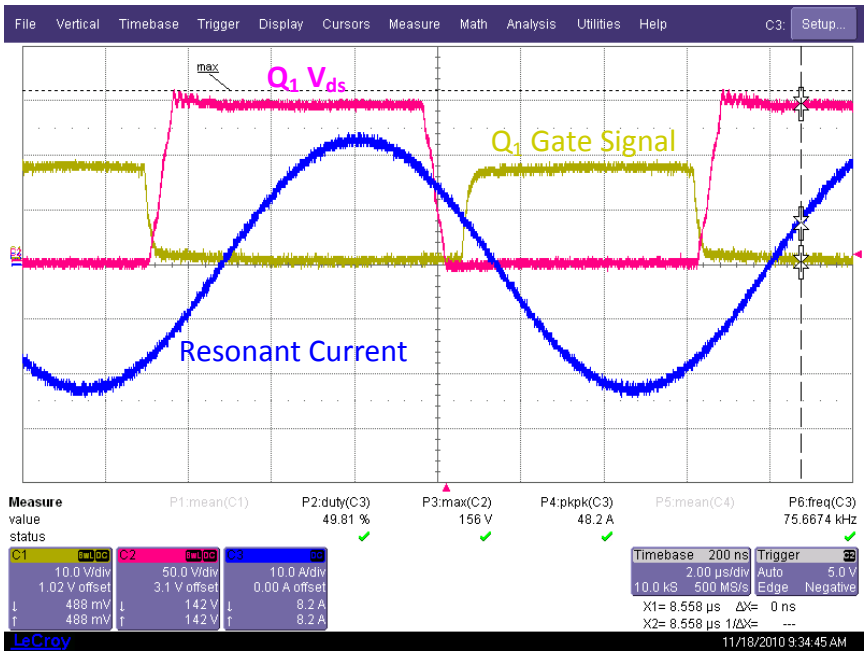

Figure 4.24 ZVS Turn-on at f=75.67 kHz for Frequency Tracking Test

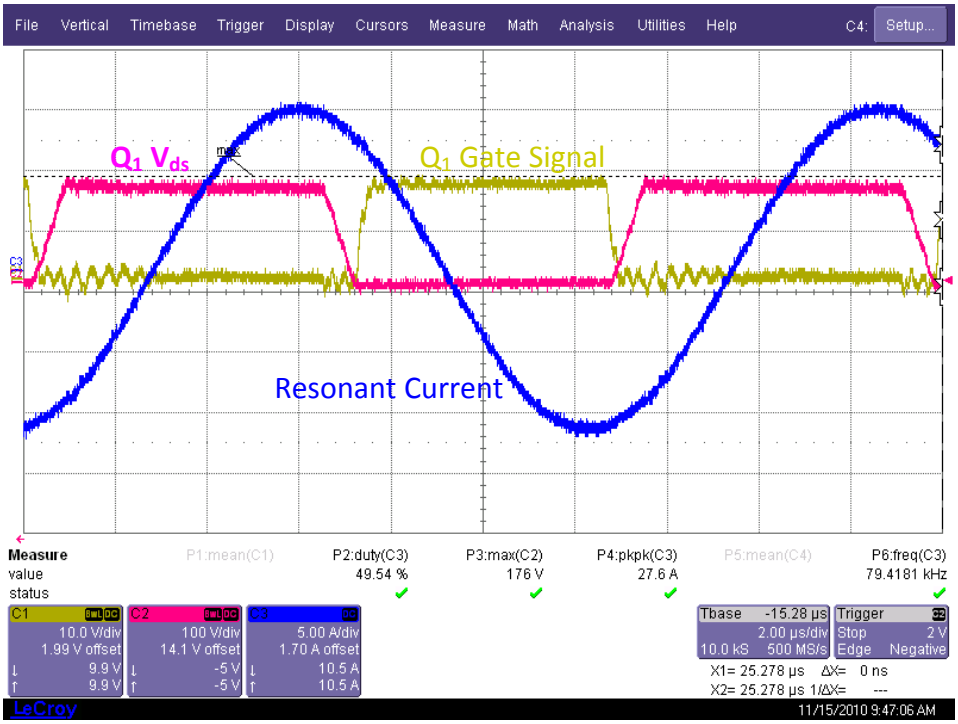

Figure 4.25 ZVS Turn-on at 300W, f=79.4kHz for Phase Shift Power Control Test

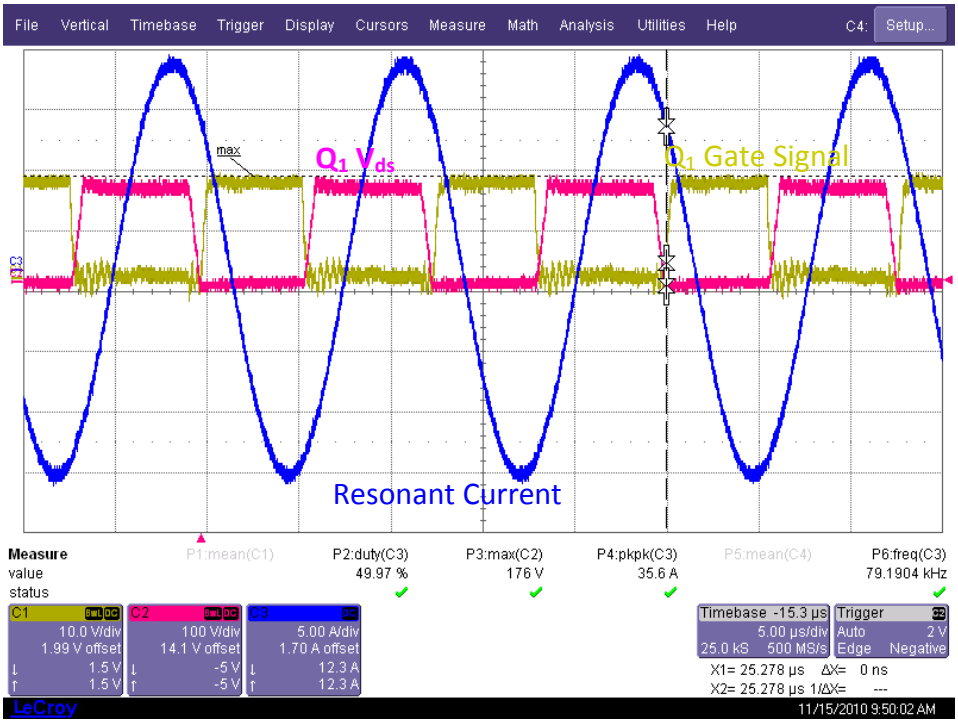

Figure 4.26 ZVS Turn-on at 500W, f=79.2kHz for Phase Shift Power Control Test

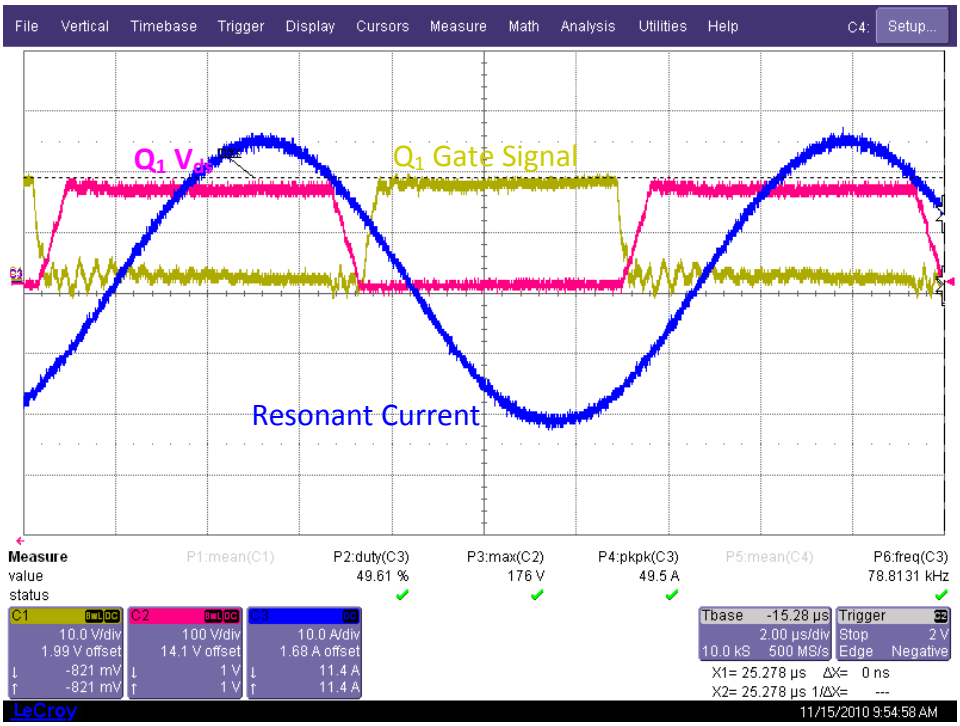

Figure 4.27 ZVS Turn-on at 920W, f=78.8 kHz for Phase Shift Power Control Test

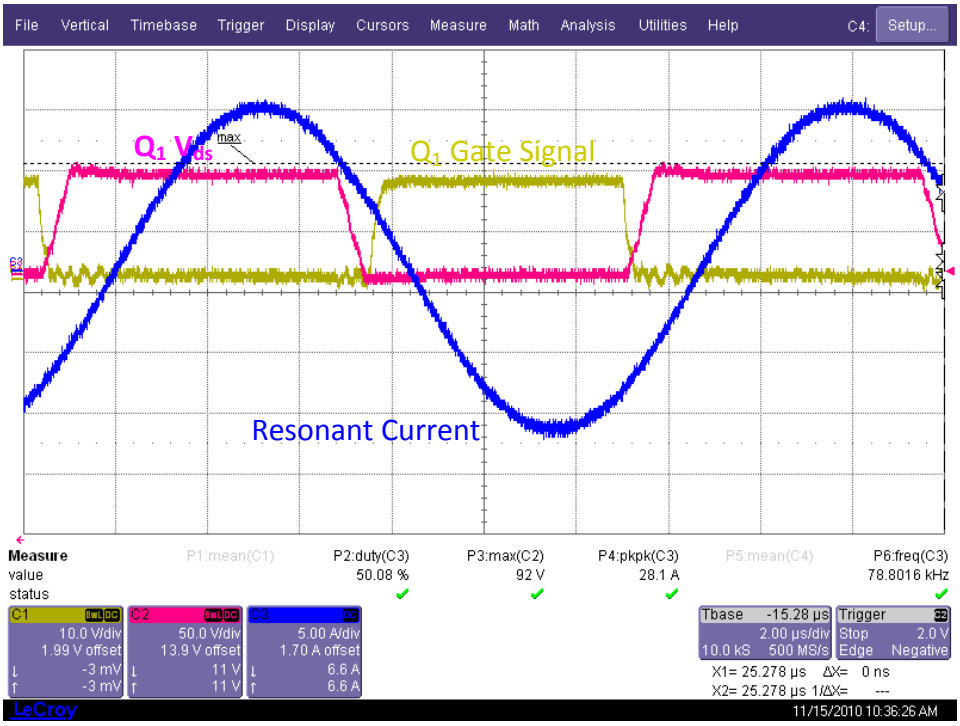

Figure 4.28 ZVS Turn-on at 290W, V=92V dc voltage control

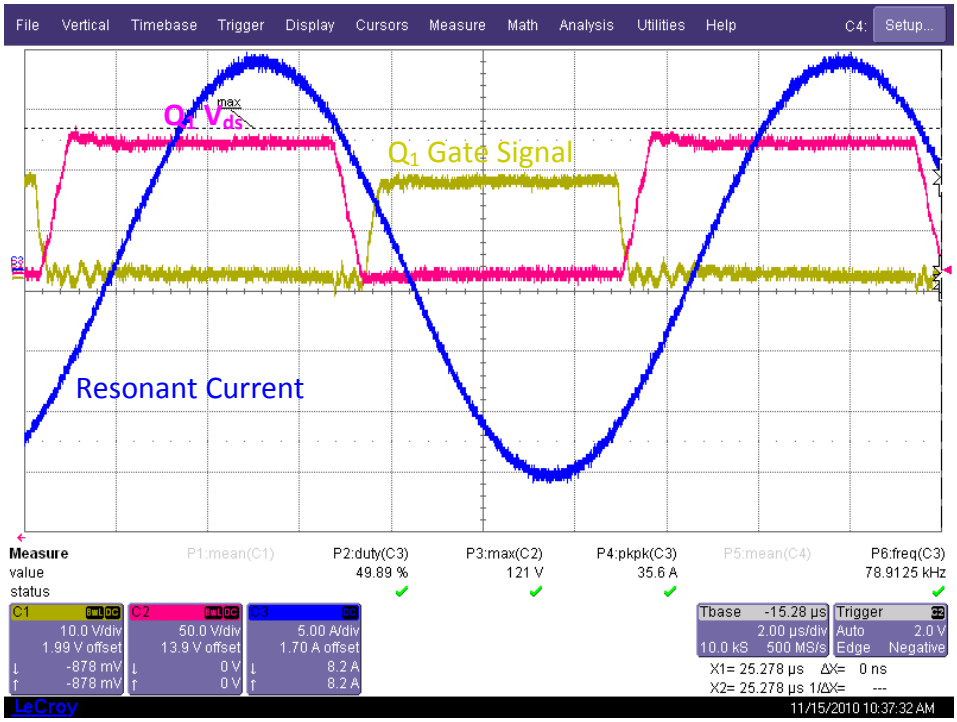

Figure 4.29 ZVS Turn-on at 500W, V=121V dc voltage control

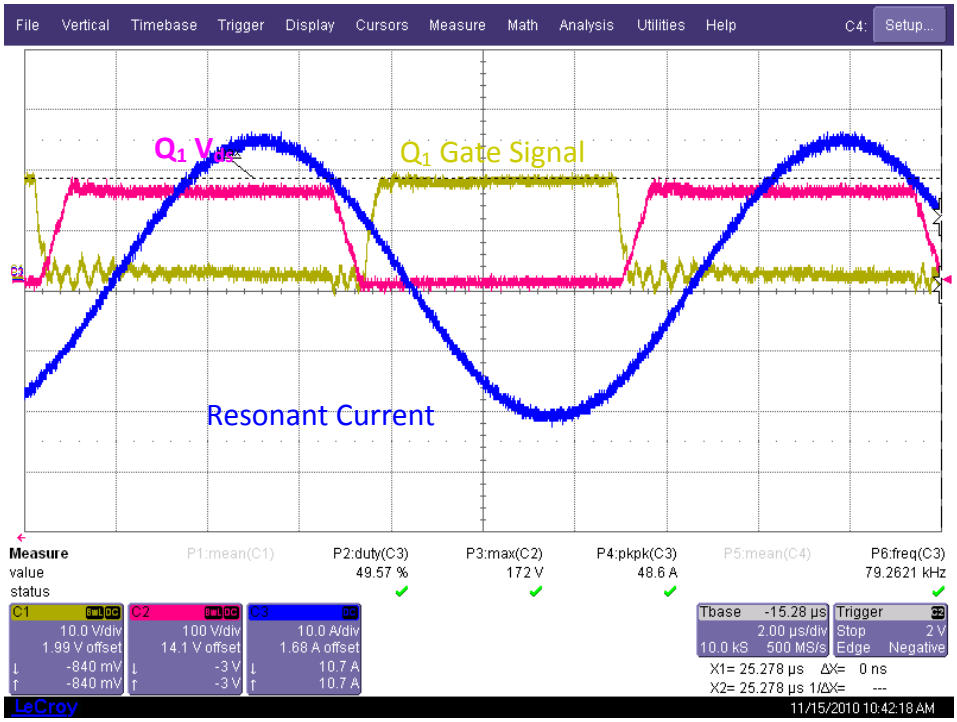

Figure 4.30 ZVS Turn-on at 890W, V=145 dc voltage control

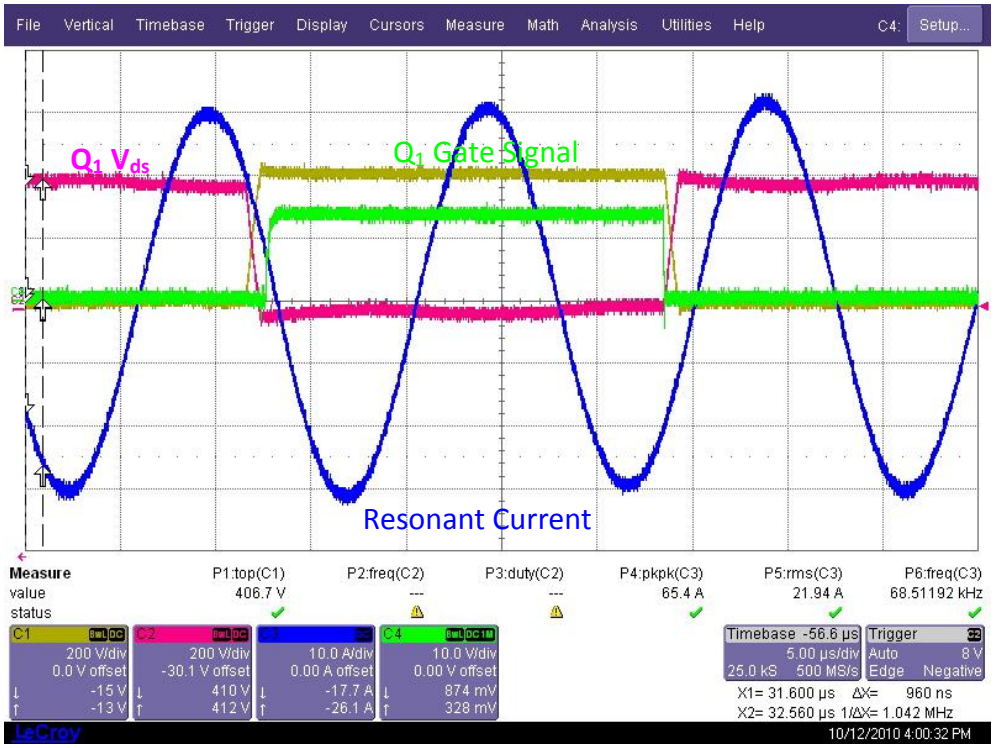

Figure 4.31 ZVS Turn-on at Vin=406.7V for triple frequency control

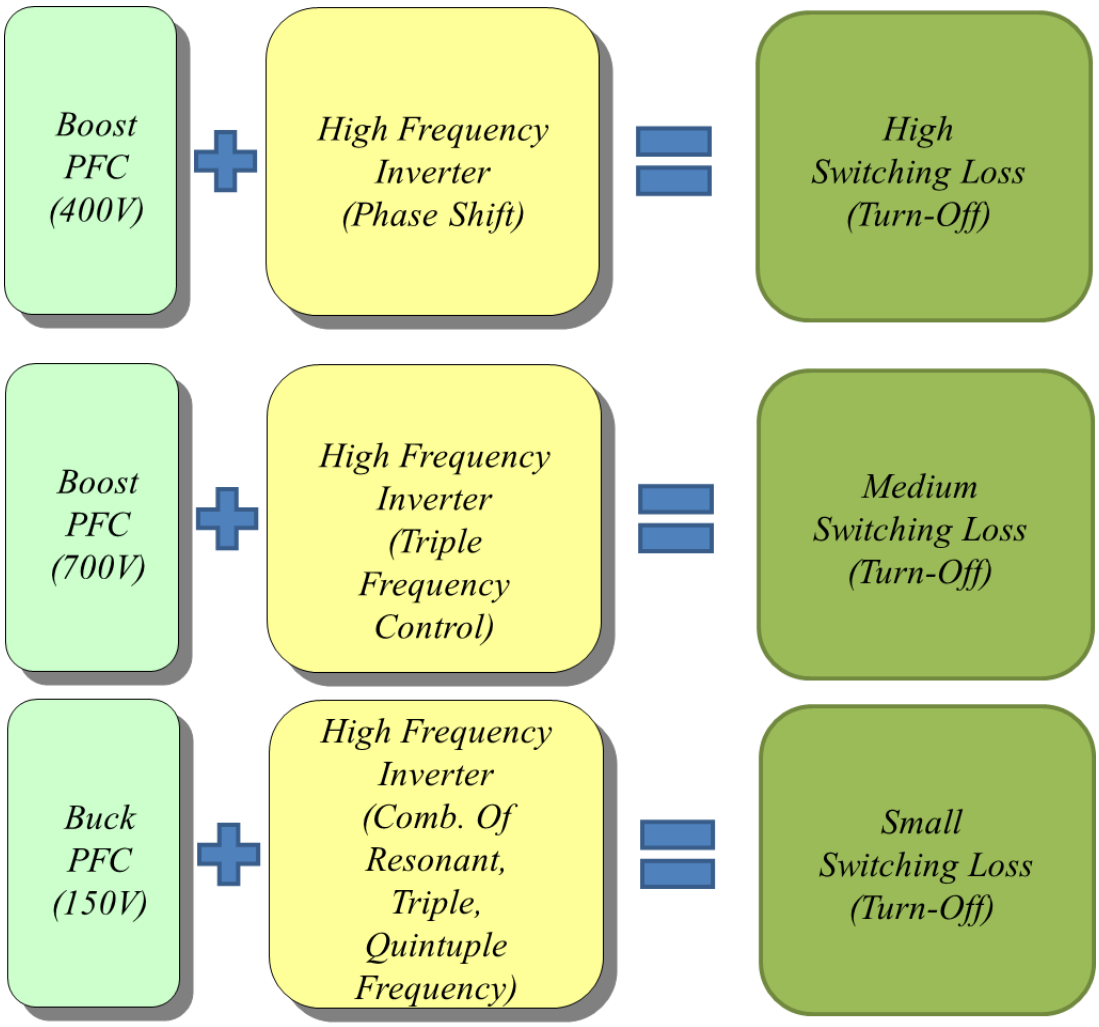

Figure 4.32 Comparison of Control Strategy

Chapter 5: Summary and Future Research

5.1 Summary

1. A review of previous articles about induction cooking and induction heating is used to understand the principles and development in the history of induction heating. Further a comprehensive comparison, analysis, and synthesis of induction heating topology is done.

2. Through the comparison of parallel resonant, series resonant inverter circuits, and single-ended type inverter, the series resonance inverter for the application of non-magnetic induction cooking is selected. Self-sustained oscillation control for load frequency tracking, as well as power adjustment is chosen. Several power control methods for combining the front-end PFC with high frequency inverter are discussed.

Through simulation and hardware implantation of the resonant inverter, the following conclusions are drawn:

(a) Despite non-magnetic material being generally low resistivity and low permeability, by increasing the induction coil's number of turns and raising the operating frequency, the cooking pan's effective resistance values can be increased, so the Joule effect is responsible for heating up the cooking pan.

(b) In order to reduce the voltage stress on the switches, the series resonant inverter topology is chosen for induction heating.

(c) The self-sustained oscillation control is used for load frequency tracking, as well as power adjustment.

(d) Combining the front-end PFC with high frequency inverter, the output power can be controlled by phase shift control, DC-link voltage control, and triple resonant frequency control. Testing results for those control methods are shown and discussed.

5.2 Future Research

(1)Further research on induction coil modeling is needed. An accurate model and simulation of induction coil using magnetic modeling software such as MAGNETS will improve an induction cooker's performance.

(2) Fixed frequency inverter control is researched. PWM control is highly desired because it has an excellent advantage of no acoustic noises being generated from its multiplex induction-heated cooking appliance unit with two or more burners for circuit operating at a fixed frequency,. General speaking, people can hear sound in 20Hz-20 kHz frequency range. Therefore, if two sounds with different frequencies interference with each other, it could generate a beat frequency, which is f=|f1-f2|

(3) Because of high operating frequency and a high quality factor of the series resonant inverter, the PCB should be laid out more carefully to make sure there is enough trace width for high current, the parasite capacitance and inductance are reduced, and there is e enough clearance and creepage for high voltage stress.

(4）Further research on inverter topology using triple, or quintuple resonant frequency is promising. Using triple/quintuple resonant frequency, the equivalent resistance of cooking pan may be increase and at the same time switching loss may be decreased. The only drawback is that the DC link voltage must be increased accordingly since the triple

resonant frequency current only produces real power with the third harmonic component of resonance voltage.

(5）It is necessary to improve the induction cooker with additional functionality, such as, overheating protection, over-current protection, overvoltage protection, power control, etc. On the other hand, when lightweight aluminum pan is used, the unit needs to automatically adjust the input power according to the weight of the aluminum pan in order to ensure the safety and reliability of the induction cooker.

Reference

[1] Zheng, Y.J., “Induction Cooker Electric Control Section Design,” M.S.’s Thesis, Zhejiang University, China, 2004.

[2] Kwon, Y.S.; Yoo, S.B.; Hyun, D.S., "Half-bridge series resonant inverter for induction heating applications with load-adaptive PFM control strategy," *Applied Power Electronics Conference and Exposition, 1999. APEC '99. Fourteenth Annual*, vol.1, pp.575-581 vol.1, 14-18 Mar 1999

[3] Koertzen, H.W.; Van Wyk, J.D.; Ferreira, J.A. , "Design of the half-bridge, series resonant converter for induction cooking," *Power Electronics Specialists Conference, 1995. PESC '95 Record, 26th Annual IEEE*, vol.2, pp.729-735 vol.2, 18-22 Jun 1995

[4] Erickson, Robert W. and Dragan Maksimovic, Fundamentals of Power Electronics, 2nd ed.; Norwell, Mass.: Kluwer Academic, c 2001. xxi, 883 p. ISBN: 0792372700 (alk. Paper); LCCN: 00052569

[5] Ahmed, S.M.W.; Eissa, M.M.; Edress, M.; Abdel-Hameed, T.S., "Experimental investigation of full bridge series resonant inverters for induction-heating cooking appliances," *Industrial Electronics and Applications, 2009. ICIEA 2009. 4th IEEE Conference on*, pp.3327-3332, 25-27 May 2009

[6] Pal, N.; Sadhu P.K.; Chakrabarti, R.N., “Choice of Pan Material in Radio-frequency Mirror Inverter Induction Cooker,” *Journal of Institution of Engineers (I)*, vol.89, pp. 09-18 March 18, 2009

[7] Tang, S.F., “A ZVS-PWM Half-Bridge DC/DC Converter: Analysis, Synthesis and Controller Design,” M.S.’s Thesis, National Cheng Kung University, Taiwan, 2003

[8] Ping, B., “Reseearch on Power Supply with Ultrahigh Frequency for Induction Heating Applications,” M.S.’s Thesis, Sichuan University, China, 2005

[9] Chu, Z.Y., “Research on 150 kHz High Power Induction Heating Power Based on IGBT,” M.S.’s Thesis, Jiangnan University, China, 2008

[10] Llorente, S.; Monterde, F.; Burdio, J.M.; Acero, J., "A comparative study of resonant inverter topologies used in induction cookers," *Applied Power Electronics Conference and Exposition, 2002. APEC 2002. Seventeenth Annual IEEE* , vol.2, pp.1168-1174 vol.2, 2002

[11] Grajales, L.; Sabate, J.A.; Wang, K.R.; Tabisz, W.A.; Lee, F.C. , "Design of a 10 kW, 500 kHz phase-shift controlled series-resonant inverter for induction heating," *Industry Applications Society Annual Meeting, 1993., Conference Record of the 1993 IEEE* , pp.843-849 vol.2, 2-8 Oct 1993

[12] *HGTG20N60A4D data sheet*, Rev. B1, Fairchild Semiconductor Corporation, Feb. 2009.

[13] *SN74S74 data sheet*, Texas Instruments, Dec.1983 (Revised Mar. 1988)

[14] Fujita, A.; Sadakata, H.; Hirota, I.; Omori, H.; Nakaoka, M., "Latest developments of high-frequency series load resonant inverter type built-in cooktops for induction heated all metallic appliances," *Power Electronics and*

Motion Control Conference, 2009. IPEMC '09. IEEE 6th International, pp.2537-2544, 17-20 May 2009

[15] Kawaguchi, Y.; Hiraki, E.; Tanaka, T.; Nakaoka, M., "Full bridge phase-shifted soft switching high-frequency inverter with boost PFC function for induction heating system," *Power Electronics and Applications, 2007 European Conference on* , pp.1-8, 2-5 Sept. 2007

[16] Wang, S.; Izaki, K.; Hirota, I.; Yamashita, H.; Omori, H.; Nakaoka, M., "Induction-heated cooking appliance using new quasi-resonant ZVS-PWM inverter with power factor correction," *Industry Applications, IEEE Transactions on* , vol.34, no.4, pp.705-712, Jul/Aug 1998

[17] Kifune, H.; Hatanaka, Y.; Nakaoka, M., "Cost effective phase shifted pulse modulation soft switching high frequency inverter for induction heating applications," *Electric Power Applications, IEE Proceedings* - , vol.151, no.1, pp. 19- 25, 9 Jan. 2004

[18] Ogiwara, H.; Itoi, M.; Nakaoka, M., "PWM-controlled soft-switching SEPP high-frequency inverter for induction-heating applications," *Electric Power Applications, IEE Proceedings* - , vol.151, no.4, pp. 404- 413, 7 July 2004

[19] Li, K.Y., “Study and Implementation of a High-Efficiency Half-Bridge Series Resonant Converter with Wide Input Voltage Range,” M.S.’s Thesis, National Taiwan University of Science and Technology, Taiwan, 2009

[20] Grajales, L., “Analysis and Design of a 500 kHz Series Resonant Inverter for Induction Heating Applications,” Ph.D.’s Dissertation, Virginia Polytechnic Institute and State University, 1995

[21] Wang, Y.W., “Research on a Novel Control System for Medium Frequency Induction Heating Power Supply,” M.S.’s Thesis, Jiangnan University, China, 2008

[22] Ni, X.L., “Research of 50kHz IGBT Series Resonance Induction Heating Power Supply” M.S.’s Thesis, Xi’an University of Technology, China, 2008

[23] Yasui, K.; Mihara, M.; Omori, H.; Nakaoka, M., "Latest Developments of Soft-Switching Pulse Modulated High Frequency Conversion Systems for Consumer Induction Heating Power Appliances," *Power Conversion Conference - Nagoya, 2007. PCC ‘07,* pp.1139-1146, 2-5 April 2007

[24] *AN9012 application note, Rev. D,* Fairchild Semiconductor Corporation, July 2003

[25] Vorperian, V., “Analysis of Resonant Converter,” PH.D.’s Dissertation, California Institute of Technology, 1984

[26] Wang, K.R.; Lee, F.C.; Hua, G.C.; Borojevic, D., "A comparative study of switching losses of IGBTs under hard-switching, zero-voltage-switching and zero-current-switching," *Power Electronics Specialists Conference, PESC '94 Record., 25th Annual IEEE* , pp.1196-1204 vol.2, 20-25 Jun 1994

[27] "About Induction Cooking," *Wikispaces*, Oct. 6, 2005. <http://inductioncooking.wikispaces.com/AboutInduction>.

[28] Rhoades, N., "A Fundamental Overview of Heating by Induction," April 22, 2006

"